MARTIN MARIETTA ENERGY SYSTEMS LIBRARIES

3 4456 0351879 9

ornl

ORNL/TM-11944

OAK RIDGE
NATIONAL
LABORATORY

MARTIN MARIETTA

Study of Radionuclides Created by ^{181}Ta (γ, *xn yp*) Reactions for Bremsstrahlung Photons Produced by 150-MeV Electrons

M. A. Miller
J. K. Dickens

OAK RIDGE NATIONAL LABORATORY
CENTRAL RESEARCH LIBRARY
CIRCULATION SECTION
4500N ROOM 175
LIBRARY LOAN COPY
DO NOT TRANSFER TO ANOTHER PERSON
If you wish someone else to see this report, send in name with report and the library will arrange a loan.
UCN-7969 (3 9-77)

MANAGED BY
MARTIN MARIETTA ENERGY SYSTEMS, INC.
FOR THE UNITED STATES
DEPARTMENT OF ENERGY

This report has been reproduced directly from the best available copy.

Available to DOE and DOE contractors from the Office of Scientific and Technical Information, P.O. Box 62, Oak Ridge, TN 37831; prices available from (615) 576-8401, FTS 626-8401.

Available to the public from the National Technical Information Service, U.S. Department of Commerce, 5285 Port Royal Rd., Springfield, VA 22161.

This report was prepared as an account of work sponsored by an agency of the United States Government. Neither the United States Government nor any agency thereof, nor any of their employees, makes any warranty, express or implied, or assumes any legal liability or responsibility for the accuracy, completeness, or usefulness of any information, apparatus, product, or process disclosed, or represents that its use would not infringe privately owned rights. Reference herein to any specific commercial product, process, or service by trade name, trademark, manufacturer, or otherwise, does not necessarily constitute or imply its endorsement, recommendation, or favoring by the United States Government or any agency thereof. The views and opinions of authors expressed herein do not necessarily state or reflect those of the United States Government or any agency thereof.

ORNL/TM-11944

Engineering Physics and Mathematics Division

Study of Radionuclides Created by ^{181}Ta $(\gamma, xn\ yp)$ Reactions for Bremsstrahlung Photons Produced by 150-MeV Electrons

M. A. Miller* and J. K. Dickens

DATE PUBLISHED — December 1991

*Student participant from the University of Wisconsin/River Falls in the student research participation program under contract number DE-AC05-76OR00033 between the U.S. Department of Energy and Oak Ridge Associated Universities.

Prepared for the
Office of Energy Research
Division of Nuclear Physics

Prepared by the
OAK RIDGE NATIONAL LABORATORY
Oak Ridge, Tennessee 37831
managed by
MARTIN MARIETTA ENERGY SYSTEMS, INC.
for the
U.S. DEPARTMENT OF ENERGY
under contract DE–AC05–84OR21400

MARTIN MARIETTA ENERGY SYSTEMS LIBRARIES

3 4456 0351879 9

CONTENTS

ACKNOWLEDGMENTS vii
ABSTRACT ix
1. INTRODUCTION 1
2. PRE-EXPERIMENTAL DETAILS 2
2.1 ESTIMATE OF RADIONUCLIDE PRODUCTION 2
2.2 ESTIMATE OF HEATING OF THE TWO-PIECE SAMPLE . . . 6
2.3 SUMMARY 10
3. EXPERIMENTAL DETAILS 11
4. DATA REDUCTION 19
5. DISCUSSION OF RESULTS 31
6. CONCLUSION 33
REFERENCES 34

LIST OF FIGURES

Fig.		Page
1	The intensity spectrum of bremsstrahlung photons created by 150 MeV electrons in Ta, calculated by the Eq. (1)	3
2	Total photon-tantalum interaction cross section vs photon energy	5
3	The above plot shows (in the shaded area) the energy region of photons having the highest probability of interacting by the $(\gamma, 1n)$ reaction	6
4	Schematic of Ta irradiation experiment	7
5	Flowchart showing the energy loss of the electron as it passes through the tantalum converter	8
6	Schematic diagram showing cylindrical volume where electrons traverse the tantalum sample and deposit energy in the form of radiation and collisions	9
7	Beam-spot location diagram	14
8	Plot of X-ray counts per second versus sample "scan" location in an attempt to define the location of the actual beam spot	15
9	Low-energy segment of the spectrum obtained commencing about 1.58 hours at the end of a 120-second irradiation of a ^{181}Ta foil by bremsstrahlung from the ORELA. Peaks are labelled with detected gamma-ray energy, in keV, and the assigned radioisotope	16
10	Next larger-energy segment of the spectrum	17
11	Highest-energy portion of the spectrum	18

Fig.		Page
12	Half life of ^{180}Ta deduced from the present experimental data for E_γ = 93 keV	21
13	Half life of ^{180m}Hf deduced from the present experimental data for $E_\gamma = 443$ keV	22
14	Half life of ^{178}Ta deduced from the present experimental data for E_γ = 1351 keV	23
15	Half life of ^{178m}Ta deduced from the present experimental data for $E_\gamma = 426$ keV	24
16	Half life of ^{177}Ta deduced from the present experimental data for E_γ = 113 keV	25
17	Half life of ^{176}Ta deduced from the present experimental data for E_γ = 1159 keV	26
18	Half life of ^{175}Ta deduced from the present experimental data for E_γ = 349 keV	27
19	Half life of ^{174}Ta deduced from the present experimental data for E_γ = 765 keV	28
20	Half life of ^{173}Ta deduced from the present experimental data for E_γ = 172 keV	29
21	Half life of ^{172}Ta deduced from the present experimental data for E_γ = 1109 keV	30

ACKNOWLEDGMENTS

We express our appreciation to D. C. Larson, J. A. Harvey, T. A. Lewis, and K. M. Wallace for active participation in the experiment, especially during the irradiation of the foils. We also thank A. L. Bangs and C. W. Glover for assistance in computer-aided preliminary documentation and S. R. Damewood and A. M. McCoy for final documentation. M. A. Miller also thanks the Oak Ridge Associated Universities for support.

ABSTRACT

Ten radionuclides, including isomers, from ^{172}Ta to ^{180}Ta and ^{180m}Hf were produced by photon interactions with a sample of elemental tantalum and measured by counting photons using a high-resolution detection system. Relative yields of these radionuclides were obtained. In addition, precision half lives were obtained for ^{175,176,180}Ta and ^{180m}Hf. Those obtained for the three Ta isotopes agree with previously reported values. For ^{180m}Hf, the present measurements resulted in a half life determination of 6.05 ± 0.06 hr, or about 10% longer than the currently adopted value for this half life.

1. INTRODUCTION

The Oak Ridge Electron Linear Accelerator (ORELA) has been a proven neutron source for many experimental research projects. Briefly, the ORELA produces a beam of electrons of nominal energy 150 MeV. The accelerated (and pulsed) electron beam strikes a target fabricated of tantalum resulting in production of bremsstrahlung. This bremsstrahlung then initiates photonuclear events in the tantalum, and the resulting neutrons have energies over a wide range from nearly thermal energies to ≈100 MeV. As part of the design phase of this accelerator, Alsmiller et al.[1] performed calculations of the expected neutron-energy fluence [i.e., N(E_n) *vs* E_n]; later Burgart et al.[2] compared measured fluences with calculated fluences for $1 < E_n < 20$ MeV showing agreement to within a factor of ~3 for this energy range. This agreement was considered very satisfactory and no further work was proposed having the goal of improving the fundamental knowledge of the photon plus tantalum interaction processes. Indeed, although measured values of cross sections have been reported[3] for Ta(γ, n) + Ta$(\gamma, 2n)$ + Ta$(\gamma, 3n)$ reactions, Alsmiller et al.[1] had to rely on calculated cross sections for total photon interactions with tantalum for $E_\gamma > 30$ MeV. A search of the literature failed to locate more recent measurements of Ta photonuclear cross sections; however, Masumoto et al.[4] reported on (γ, n), $(\gamma, 2n)$, and $(\gamma, 3n)$ cross sections for bremsstrahlung E_γ to 70 MeV and for several heavy elements (Au and Pb). It is of some interest, then, to initiate a study of photon interactions with Ta not only for specific application of neutron production in the ORELA target but also leading to a further understanding of the fundamental nuclear processes involved in this reaction.

There is, in addition, a very pragmatic reason for this study, and that is to quantify the build up of radionuclides in the target. With this knowledge, maintenance scheduling can be better planned. In addition, the types and amounts of materials needed for shielding used targets can be better estimated.

The present experiment was meant to be of a scoping nature. The experimental configuration, an air-cooled radiator foil (0.051-cm Ta) preceeding the sample foil (0.0075-cm Ta), had never been tried before, and we were concerned if enough radionuclide yield could be made in the sample without damage to the radiator foil by the impinging electron beam. Consequently, a careful pre-experiment analysis was conducted, and this analysis is discussed in some detail in the next section. This analysis indicated that the experiment could be carried out, and the following sections detail the experiment and presents our results. Finally, conclusions and recommendations for further work are given.

2. PRE-EXPERIMENTAL DETAILS

2.1 ESTIMATE OF RADIONUCLIDE PRODUCTION

Before the actual experiment was run, it was necessary to determine how long the irradiation should last. The first question to be answered was whether or not the irradiation would produce a sufficient amount of radioactivity. We started with the assumption[5] that at a maximum power of 50 kilowatts, approximately 10^{16} bremsstrahlung photons/sec were produced in the ORELA tantalum target.[†] For the present experiment, the ORELA was to run at about 1 kilowatt, and thus the bremsstrahlung production should drop by a factor of 50:

$$\text{photons/sec} = \frac{1}{50} \times 10^{16} = 2 \times 10^{14}$$

When an electron travels through a material, the radiation length of that material is defined to be the distance over which the electron energy is reduced by a factor $1/e$. Given that the radiation length in tantalum is 0.3823 cm,[1] it is reasonable to assume that electrons travelling through the ORELA tantalum target will lose nearly all their energy in the form of bremsstrahlung photons since the target itself is very thick. However, the bremsstrahlung necessary for the experiment was to be produced in a tantalum converter having a thickness of only 0.051 cm. One may determine[6] that approximately 12.3% of the electron energy incident on the tantalum converter would be converted into bremsstrahlung photons. Therefore, the bremsstrahlung production in the tantalum converter should be, to a good approximation:

$$0.123 \times (2 \times 10^{14}) = 2.46 \times 10^{13} \text{ photons/sec}$$

Now that the estimate of the number of bremsstrahlung photons produced was complete, it was necessary to determine the intensity of the photons at a given energy, or in other words, the bremsstrahlung spectrum. The following equation from Johns et al.[7] gives the relative intensity of the bremsstrahlung in the forward direction:

$$\Gamma(E, E_0) = 8[2(1-z)(\ln\ \alpha - 1) + z^2(\ln\ \alpha - 0.5] \qquad (1)$$

[†] This statement is not strictly correct unless a photon-energy threshold is defined. The bremsstrahlung production becomes large and ill defined as $E_{photon} \rightarrow zero$. However, the energy spectrum, $E_{photon} \times N(E_{photon})$, is finite as $E_{photon} \rightarrow zero$. For the pre-analysis given in this section we have assumed (a) a low photon-energy threshold not specifically defined but small compared to our photon energies of interest and (b) an essentially constant thin-radiator bremsstrahlung spectrum. Then any change in the photon yield will result in an equivalent change in the energy yield (and vice versa), and the analysis in this section may be carried out as given.

where

$$\alpha^2 = \frac{\alpha_1^2 \alpha_2^2}{\alpha_1^2 + \alpha_2^2}$$

$$\alpha_1 = 2E_0(1-z)/\mu z$$

$$\alpha_2 = 191/Z^{1/3}$$

Here, $\Gamma(E, E_0)$ is the intensity, μ is the rest energy of the electron, E is the energy of the photon, $z = E/E_0, E_0$ is the total energy of the electron, and Z is the atomic number of the target material. Evaluating Eq. (1) for 150-MeV electrons incident on tantalum for photon energies ranging from 0 to 150 MeV yields the bremsstrahlung spectrum shown in Fig. 1.

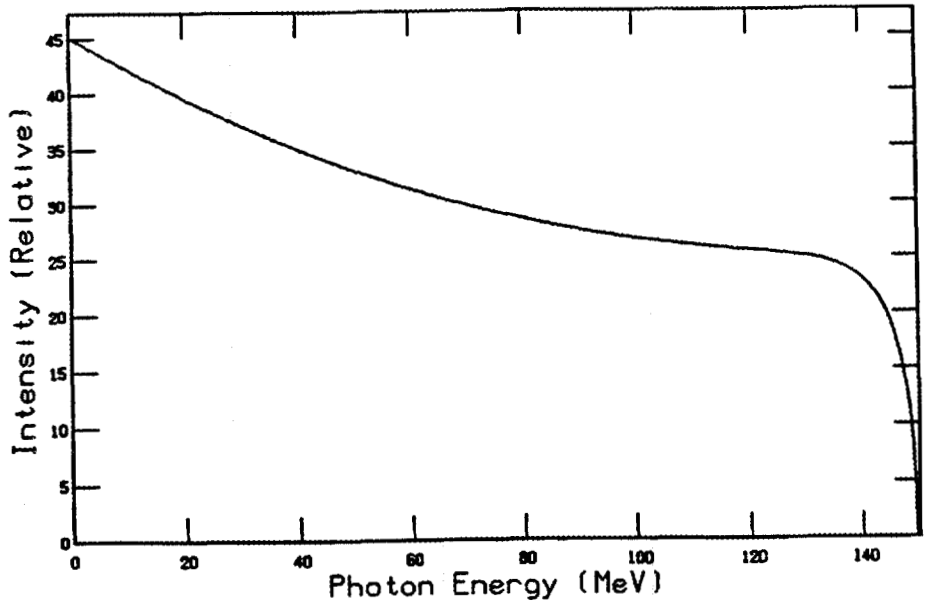

Fig. 1. The intensity spectrum of bremsstrahlung photons created by 150 MeV electrons in Ta, calculated by the Eq. (1).

The calculated intensity spectrum of Fig. 1 does not exhibit the expected $1/E$ dependence. In fact, if one defines a function $N(E, E_0)$ as the number of photons of energy E per unit photon energy interval, then[8]

$$N(E, E_0) = F(E_0)\Gamma(E, E_0)/E \tag{2}$$

where $F(E_0)$ is a normalizing parameter. To complete the actual experimental description of $N(E, E_0)$ the right-hand side of equation (2) should also include a photon attenuation function, $a(E)$. However, the photon attenuation in the present experiment is small and has essentially no effect on the final results.

Table 1. Q-Values for ^{181}Ta$(\gamma, xn)^{181-x}$Ta reactions for $x = 1$ to 11

Reaction	Q-value[a]
^{181}Ta$(\gamma, 1n)^{180}$Ta	7.577 ± 0.001
^{181}Ta$(\gamma, 2n)^{179}$Ta	14.222 ± 0.005
^{181}Ta$(\gamma, 3n)^{178}$Ta	22.10 ± 0.10
^{181}Ta$(\gamma, 4n)^{177}$Ta	28.975 ± 0.010
^{181}Ta$(\gamma, 5n)^{176}$Ta	37.30 ± 0.10
^{181}Ta$(\gamma, 6n)^{175}$Ta	44.50 ± 0.10[b]
^{181}Ta$(\gamma, 7n)^{174}$Ta	53.07 ± 0.10[b]
^{181}Ta$(\gamma, 8n)^{173}$Ta	60.61 ± 0.22[b]
^{181}Ta$(\gamma, 9n)^{172}$Ta	69.60 ± 0.19
^{181}Ta$(\gamma, 10n)^{171}$Ta	77.60 ± 0.20[b]
^{181}Ta$(\gamma, 11n)^{170}$Ta	86.88 ± 0.20[b]

[a]Based on the 1983 mass evaluation of Wapstra and Audi (ref. 9).
[b]Mass values and uncertainties based on "systematics" in Wapstra and Audi (ref. 9).

The next step in our analysis was to determine photon-energy thresholds for the potential (γ, xn) reactions to be observed. The 1983 evaluation of Wapstra and Audi[9] gives Q values for the $(\gamma, 1n)$ and $(\gamma, 2n)$ reactions. Q values for (γ, xn) where $x \geq 3$ were computed from the masses given in this evaluation, and these Q values are given in Table 1.

It was expected that the $(\gamma, 1n)$ reaction would dominate over all others since it has the lowest threshold energy. Figure 2, taken from Alsmiller et al.,[1] shows how the cross section for the total (γ, xn) reaction varies with photon energy.

As can be seen in Fig. 2, the experimental cross section for the (γ, xn) reaction is largest around 10 to 20 MeV. This portion of the total (γ, xn) cross section is due primarily to the $(\gamma, 1n)$ reaction. Thus, the important part of the bremsstrahlung curve for the $(\gamma, 1n)$ reaction is shown approximately by the shaded region in Fig. 3.

The shaded area encloses about 9% of the total number of bremsstrahlung photons. Thus,

$$N_\gamma = \text{ photons available to interact} \simeq 0.09 \times 2.46 \times 10^{13} \text{ photons/sec}$$
$$\simeq 2.2 \times 10^{12} \text{ photons/sec}$$

With an estimate of the spot size of the beam to be about 2 cm in diameter, the total number of tantalum nuclei in the thin foil irradiated by the beam was determined to be 4.2×10^{20} nuclei/cm^2. Using an average value $\sigma = 200$ millibarns

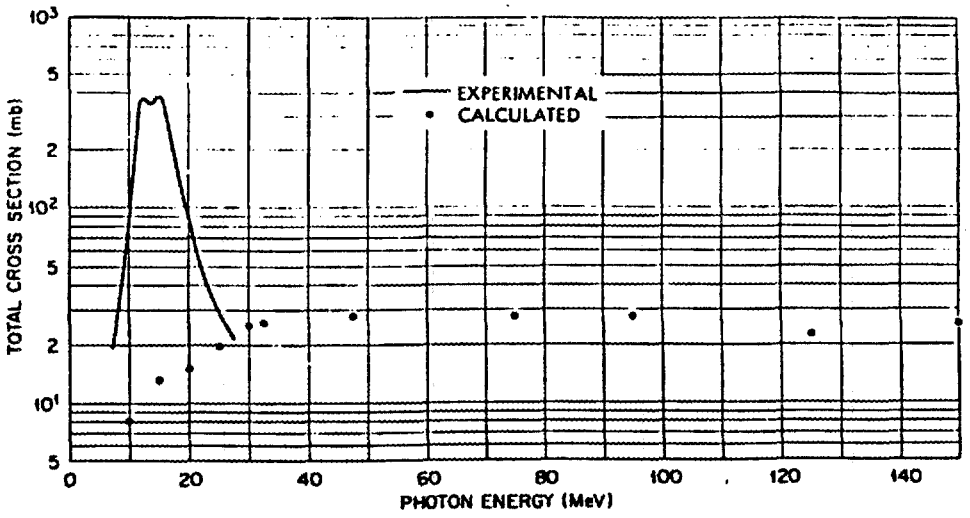

Fig. 2. Total photon-tantalum interaction cross section vs photon energy. The solid line represents the experimental data of ref. 3, and the dots indicate calculated values by Alsmiller et al. (ref. 1).

(1 barn = 10^{24} cm^2) for the cross section of the $(\gamma, 1n)$ reaction taken from Fig. 2 led to the following determination of the expected yield of the reaction:

$$\text{Yield of } (\gamma, 1n) \text{ reaction} \approx 4.2 \times 10^{20} \text{ nuclei/cm}^2 \times \sigma \times N_\gamma$$
$$\approx 1.8 \times 10^8 \text{ atoms/sec of irradiation}$$

From experimental results by Masumoto et al.[4], the expected yield of other photoneutron reactions appears to decrease successively by a factor of about 4 for each additional emitted neutron, meaning that the expected yield of the $(\gamma, 2n)$ should be around 4.5×10^7 atoms/sec and the $(\gamma, 3n)$ about 1.1×10^7 atoms/sec.

The effects of radioactive decay on the yield of these freshly created isotopes was also considered. Assuming that the half-life of a typical nuclide created in the (γ, xn) reaction to be around 20 minutes, then the rate at which the nuclide decays is given by

$$\frac{dN}{dt} = \lambda N = (5.8 \times 10^{-4} \text{ s}^{-1})(1.8 \times 10^8 \text{ atoms/sec}) \approx 1.1 \times 10^5 \text{ decays/sec} ,$$

where $\lambda = \ln\ 2/t_{1/2}$. A quick glance at the Chart of the Nuclides[10] shows that most of the Ta isotopes lighter than ^{181}Ta have half-lives on the order of hours or more, and thus if they were created during the irradiation they should be detectable.

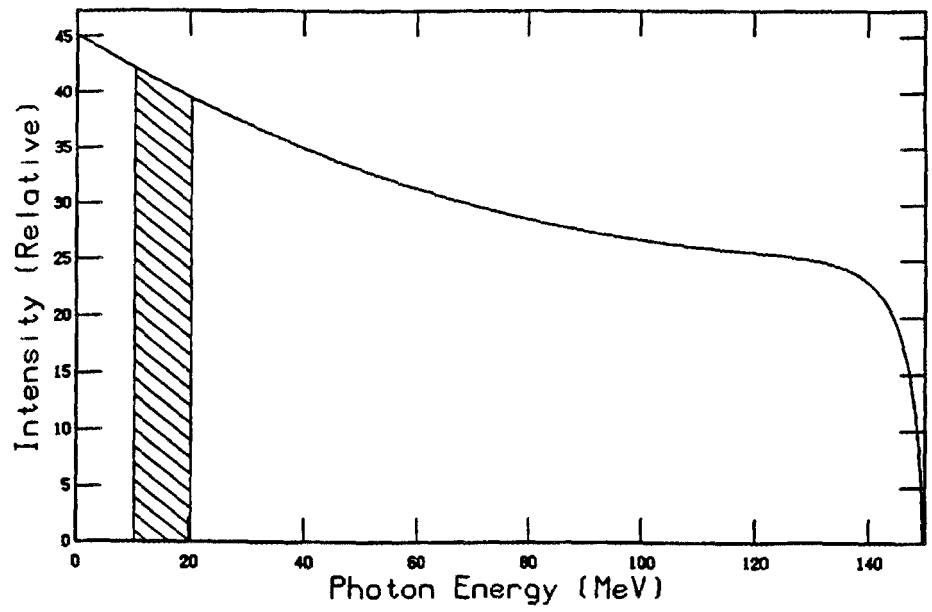

Fig. 3. The above plot shows (in the shaded area) the energy region of photons having the highest probability of interacting by the $(\gamma, 1n)$ reaction.

2.2 ESTIMATE OF HEATING OF THE TWO-PIECE SAMPLE

The experimental configuration is schematically illustrated in Fig. 4. Cooling of the sample by any conventional methods such as water circulation was not available at the time of this experiment, and thus only the surrounding air in the target room served to transfer heat away from the sample. The second question that had to be resolved was in regard to the physical heating of the sample during the irradiation. The major concern was not that the electron beam would burn a hole in the sample, but rather that the sample would reach a temperature (about 600°C) at which the formation of tantalum pentoxide (Ta_2O_5) would be initiated. Such oxidation of the sample during the irradiation could mean a loss of sample material, since oxidized pieces of the sample could flake and fall off. Therefore, estimates had to be made of the rate at which both the Ta converter and the Ta foil would heat up.

The stopping power for 150-MeV electrons in tantalum is estimated[6] to be about 21 MeV/cm^2/gm. Since the electron beam contacts the 0.051-cm-thick converter first, the energy loss experienced by an electron in passing through it is 17.7 MeV. This is roughly 12% of the initial electron energy, and thus if the entire beam power is 1000 watts, then 120 watts would be removed from the beam by the tantalum converter. The electron energy loss can be divided into radiation (bremsstrahlung) losses and collisional losses. For high-energy electrons such as the ones produced at ORELA, the energy losses due to bremsstrahlung dominate over the collisional losses. The following formula from Turner[11] gives the "radiation yield" for electrons of kinetic energy T impinging upon a material of atomic number Z:

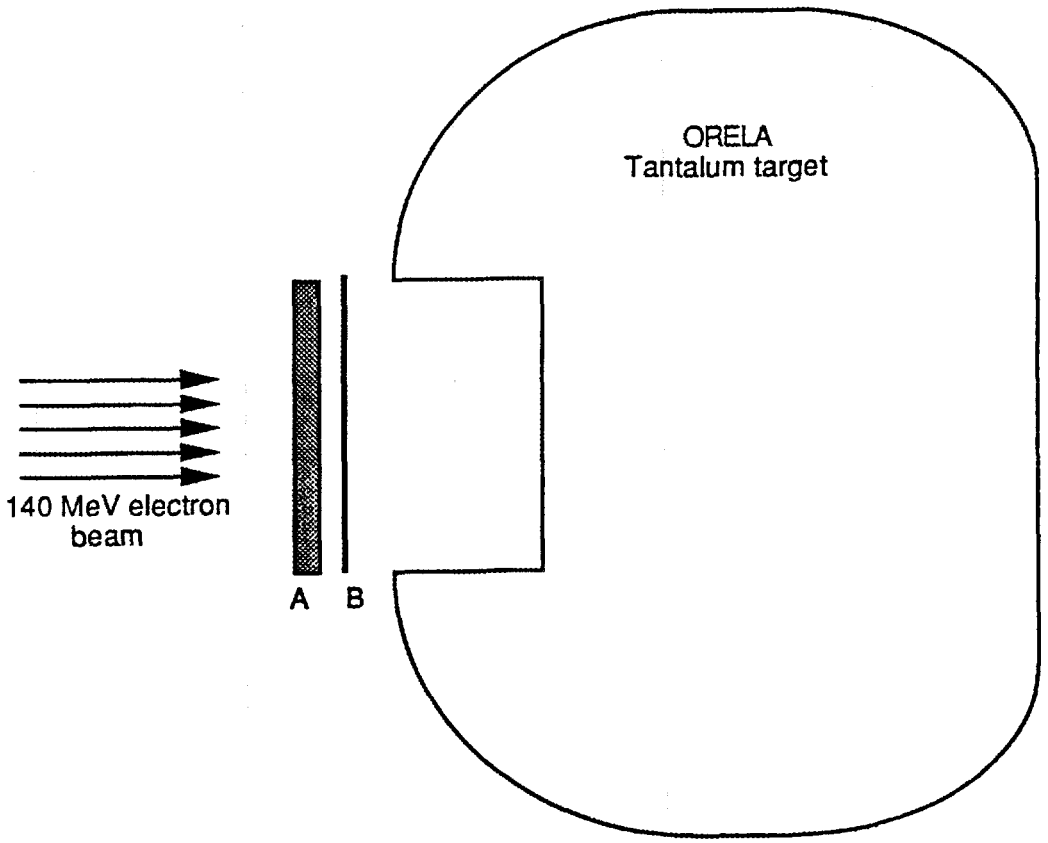

Fig. 4. Schematic of Ta irradiation experiment. The electron beam incident from the left impinged on a Ta converter (A) of thickness 0.051 cm which resulted in the production of bremsstrahlung radiation in the forward direction. These photons then interacted with the thin Ta foil (B) of thickness 0.0076 cm by means of the ^{181}Ta$(\gamma, xn\ yp)$ reaction.

$$Y = \text{ radiation yield} \simeq \frac{6 \times 10^{-4} Z\,T}{1 + 6 \times 10^{-4} Z\,T}$$

For an electron of kinetic energy $T = 150$ MeV in tantalum ($Z = 73$), the radiation yield is 0.87. Thus, of the 120 watts deposited in the tantalum converter 87% takes the form of bremsstrahlung photons and the other 13% is of the form of collisional losses. However, not all of the bremsstrahlung will interact with the tantalum. Low-energy photons interact primarily by the photoelectric effect and deposit all their energy. Photons of intermediate energy that do not interact by the (γ, xn) reaction tend to undergo Compton scattering and may or may not deposit all their energy in the sample. High energy photons have a higher cross section for pair production, and thus deposit most of their energy in that manner. Since the photons are produced throughout the sample, the "average" distance travelled by a photon in passing through it is taken to be half the sample thickness. In the case of

the 0.051-cm-thick tantalum converter, this average distance is 0.0255 cm. How far a given photon will penetrate is governed statistically by a probability of interaction per unit distance travelled, which depends on the medium traversed and on the photon energy. The probability per unit distance travelled that a photon interacts by one physical process or another is denoted by μ, the linear attenuation coefficient. The linear attentuation coefficient for tantalum on the average for photon energies of 150 MeV is $\mu \cong 1.49$ cm^{-1}. If I_0 is the incident photon intensity, then after traversing a distance x through a material with linear attenuation coefficient μ, the resulting photon intensity is given by:

$$I = I_0 e^{-\mu x} = I_0 e^{(-1.49)(0.0255)} = 0.963\ I_0$$

Thus, only about 3.7% of the bremsstrahlung produced actually interact by some mechanism in the tantalum converter. A "flowchart" depicting the loss of electron energy as it passes through the tantalum is shown in Fig. 5.

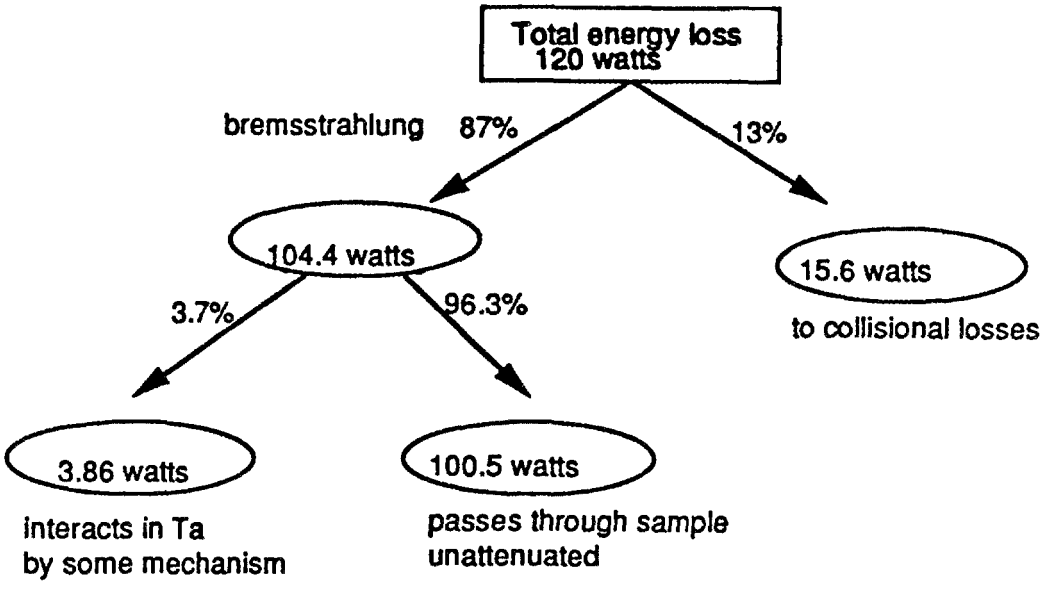

Fig. 5. Flowchart showing the energy loss of the electron as it passes through the tantalum converter.

The temperature change when an amount of heat energy Q is deposited in a material of mass m and specific heat c is given by Halliday and Resnick[12] to be

$$\Delta T = \frac{Q}{mc} \tag{3}$$

Using Eq. (3), the temperature rise in the region of the converter struck by the electron beam was expected to be $\approx 53°/\text{sec}$, in the absence of any cooling.

The actual temperature rise was dependent on how much the converter would cool due to (a) black-body radiation emission and (b) heat conduction into the body of the sample. As the sample heats up, it behaves like a black-body radiator, radiating energy at a rate proportional to the fourth power of its temperature. Calculations of black-body emissions were determined for a sample temperature of 850 K, which is just below the oxidation temperature of 873 K. The calculations predicted only 9.3 watts of cooling for the converter due to black-body radiation.

Heat conduction played a more significant role. The heat energy is deposited in a cylindrical volume of the sample with the radius of the beam spot defining the radius of the "cylinder" (see Fig. 6).

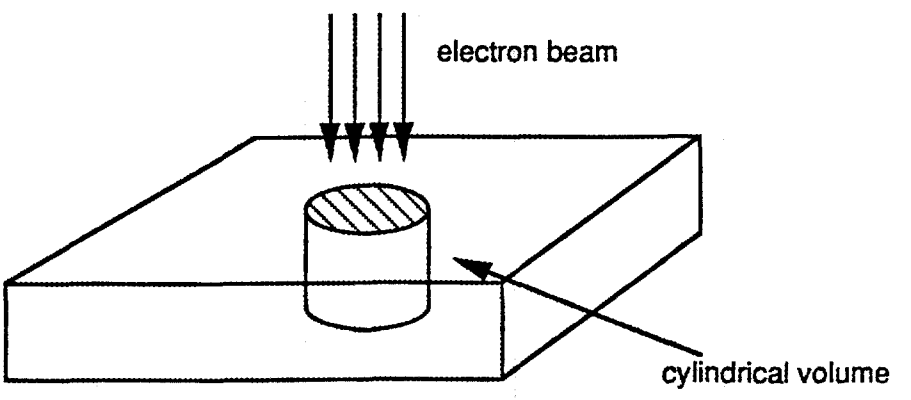

Fig. 6. Schematic diagram showing cylindrical volume where electrons traverse the tantalum sample and deposit energy in the form of radiation and collisions.

The surface area of the sides of the "cylinder" pictured above for the 0.051-cm-thick converter is

$$A = \pi(2 \text{ cm})(0.051 \text{ cm}) = 0.32 \text{ cm}^2 \ .$$

The equation governing the conduction of heat through the converter is given by Halliday and Resnick[12] to be:

$$\frac{\Delta Q}{\Delta t} = K \ A \ \frac{\Delta T}{L}$$

where

$$\begin{aligned} \Delta t &= \text{time (1 second)} \\ \Delta Q &= \text{heat energy transferred} \\ K &= \text{thermal conductivity (0.5 watts/cm}^2\text{/sec)} \\ \Delta T &= 53°\text{C} \\ L &= 0.1 \text{ cm} \end{aligned}$$

Solving for ΔQ, the heat energy transferred gives $\Delta Q = 85$ watts/sec, a value larger than the 19.5 watts/sec deposited in the foil. Thus, the body of the sample will absorb the electron energy deposited. The mass of the irradiated area is 2.65 gm and the mass of the entire converter is about 38.2 gm. Since the entire converter is about 14 times as massive as the irradiated volume, the temperature rise would be expected to be:

$$(50°\text{C/sec})/14 \cong 3.5°\text{C/sec.}$$

A similar type of analysis was done for the thin foil, and it was found by comparison that the Ta converter absorbed a greater portion of the incident electron beam energy. Thus, it was desired to keep the temperature rise of the converter to a minimum.

2.3 SUMMARY

The expected rate of temperature increase, coupled with the expected yield of the reaction products per second, suggested that a continuous irradiation of about 100 seconds would be sufficient to induce enough radioactivity by photo-nuclear reactions and still prevent oxidation of the sample.

3. EXPERIMENTAL DETAILS

Because of limitations imposed at the time of the irradiation, primarily safety considerations but also because of a mechanical fault of the ORELA target system at the time of measurement, the irradiation configuration had to be designed to use the then existing ORELA target configuration. The Ta converter and thin foil were mounted onto the ORELA target using thin aluminum rods in the orientation shown in Fig. 4. The 150-MeV electron beam produced by the ORELA first struck a Ta converter of thickness 0.051 cm, resulting in the production of bremsstrahlung radiation in the forward direction. This bremsstrahlung radiation then went on to interact by means of the (γ, xn yp) reaction in a 0.0076-cm-thick Ta foil. The irradiation of the foil at 1 kilowatt of beam power lasted for 120 seconds.

To measure the increase in temperature, a thermocouple was attached to the converter at a location just outside of the expected incident beam spot. The thermocouple was monitored by personnel outside the accelerator room using an electronic meter connected to the thermocouple by means of a long wire. The initial temperature of the Ta converter was 25°C and it rose to 67°C by the end of the 120-second irradiation. Thus, the rate at which the converter heated was less than the 3.8°C/sec that was expected. This temperature rise as recorded by the thermocouple may not be an accurate value, however. There is evidence, discussed below, that the electron beam struck the Ta converter above the expected spot, meaning that the actual temperature rise of the converter was probably greater than the 42°C recorded by the thermocouple. Nevertheless, no oxidation or discoloration of the sample occurred.

At the end of irradiation, the foil and converter were retrieved from the target room and briefly monitored for radioactivity. After it had been determined that the sample had enough activity for analysis, it was transported in a lead pig to a laboratory equipped with two γ-ray detector systems, each of high-purity germanium. The thin sample foil was removed from the pig and initially placed on the 20-cm level of the detector ladder and lowered into the lead cave containing a Ge(Li) detector. The analyzer was activated and a short 10-second data acquisition was taken for the purpose of determining the dead time of the detector. Since the dead time was found to be only about 5%, the sample was moved to the 10-cm level where the dead time was a reasonable 13%. A sequence of data acquisitions ensued, consisting of 60, 90, 90, 90, 120, 120, 150, and 150 seconds in length. These short acquisition times were intended to record the gamma emissions of any short-lived radioisotopes created in the irradiation. The total amount of time elapsed from the end of the irradiation to the start of data acquisition was about six minutes.

The times of the data acquisitions grew longer and longer after the initial eight, and as of this writing approximately 65 spectra have been recorded over a 28-day period. The information on the spectra relevant to data taken on the thin foil is given in Table 2.

Table 2. Record of Data Gathered in Ta Irradiation Experiment

Run number	Cooling time (seconds)	Real time (seconds)	Live time (seconds)	Detector Type[a]	Distance (cm)
1	360	63	60	Ge(Li)	20.5
2	430	95	90	Ge(Li)	20.5
3	810	68	60	Ge(Li)	10.5
4	882	102	90	Ge(Li)	10.5
5	990	102	90	Ge(Li)	10.5
6	1095	101	90	Ge(Li)	10.5
7	1200	134	120	Ge(Li)	10.5
8	1339	133	120	Ge(Li)	10.5
9	1477	166	150	Ge(Li)	10.5
10	1648	165	150	Ge(Li)	10.5
11	1943	328	300	Ge(Li)	10.5
12	2316	392	360	Ge(Li)	10.5
13	2822	487	450	Ge(Li)	10.5
14	3339	592	550	Ge(Li)	10.5
15	4069	643	600	Ge(Li)	10.5
16	4735	961	900	Ge(Li)	10.5
17	5715	1273	1200	Ge(Li)	10.5
18	7140	1267	1200	Ge(Li)	10.5
19	8433	1576	1500	Ge(Li)	10.5
20	10002	1882	1800	Ge(Li)	10.5
21	12810	2244	2160	Ge(Li)	10.5
22	16480	2477	2400	Ge(Li)	10.5
23	18960	2777	2700	Ge(Li)	10.5
24	21750	3076	3000	Ge(Li)	10.5
25	24830	3680	3600	Ge(Li)	10.5
26	28520	3669	3600	Ge(Li)	10.5
27	32190	4272	4200	Ge(Li)	10.5
28	36470	4870	4800	Ge(Li)	10.5
30	63180	7200	7131	Ge(Li)	10.5
31	70870	7376	7316	Ge(Li)	10.5
32	78430	9186	9125	Ge(Li)	10.5
33	89220	10042	10000	Ge(Li)	10.5
34	99270	10034	10000	Ge(Li)	10.5
35	109300	10029	10000	Ge(Li)	10.5
36	119300	10023	10000	Ge(Li)	10.5
37	129400	10020	10000	Ge(Li)	10.5
38	139400	10017	10000	Ge(Li)	10.5
39	149500	11009	10994	Ge(Li)	10.5
40	161600	18022	18000	Ge(Li)	10.5
42	197700	18016	18000	Ge(Li)	10.5
43	215700	18014	18000	Ge(Li)	10.5
44	233700	18013	18000	Ge(Li)	10.5
45	251800	18012	18000	Ge(Li)	10.5
46	270900	24014	24000	Ge(Li)	10.5
47	294900	24015	24000	Ge(Li)	10.5
48	319740	37064	37050	LEPS	5.5
50	357900	24014	24000	Ge(Li)	10.5

Table 2. Continued

Run number	Cooling time (seconds)	Real time (seconds)	Live time (seconds)	Detector Type[a]	Distance (cm)
51	381360	24013	24000	Ge(Li)	10.5
52	405500	40300	40275	LEPS	5.5
53	451068	41147	44101	Ge(Li)	3.0
54	510270	70258	70200	Ge(Li)	3.0
55	591690	87732	87700	LEPS	5.0
56	698160	93975	93900	Ge(Li)	3.0
57	793470	84860	84800	Ge(Li)	3.0
59	871400	78430	78400	LEPS	5.0
61	957800	87144	87100	LEPS	5.0
63	1049000	134102	134007	Ge(Li)	3.0
65	1183320	180512	180404	Ge(Li)	3.0
68	2365220	164627	164518	Ge(Li)	3.0
74	1821320	60827	60855	LEPS	5.0
75	1907680	232092	232199	LEPS	5.0
76	2166990	65000	65030	LEPS	5.0
77	2255250	62000	62029	LEPS	5.0
79	2320470	79700	79727	LEPS	5.0

[a]Ge(Li) is a large-volume detector. LEPS is a Low-Energy Photon detector.

Two detectors were used to gather data, the Ge(Li) and a LEPS detector. The Ge(Li) detector recorded gamma energies up to 2800 keV while the LEPS detector measured low energy gammas (energies less than about 400 keV) with the better resolution. In the LEPS, the sample was placed at the 5-cm source-to-detector level. Since the true location of the beam spot was not near the middle of the sample as expected, a correction to the final yields of radionuclides determined using LEPS data was needed. Also, looking at Table 2, the source-to-detector distances corresponding to runs 1–52 all have an additional 0.5 cm added on. This was necessary because the sample was not flat initially but was bowed slightly, and the estimated curvature was 0.5 cm. For the runs past No. 52, the sample was physically flattened so that the addition of 0.5 cm was no longer necessary.

The actual location of the beam spot on the Ta sample was determined by fashioning a small hole (≈5 mm diameter) in a thin (1-mm thick) lead sheet and placing the hole over the LEPS detector. The thin Ta foil was then scanned to find out where the sample was "hottest" by examining the number of main Ta X-rays collected from different places on the foil. Thermal-neutron-induced ^{182}Ta was also present in the sample, and the 100-keV gamma from it was also counted as a reference since it was present in relatively constant amounts throughout the foil. A diagram showing the foil and the expected and actual locations of the center of the beam spot is given in Fig. 7.

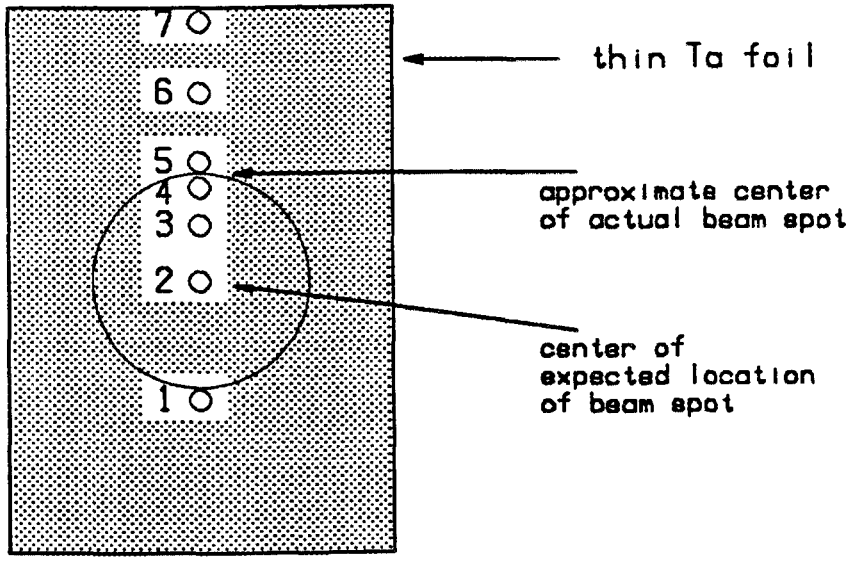

Fig. 7. Beam-spot location diagram. It was anticipated that the photon-induced radioactivity would be well inside the circle shown in the figure. To check this assumption, the sample was scanned as described in the text. The numbered points represent locations at which the sample was scanned for radioactivity level. These numbers correspond to the trial numbers given in Table 3.

The results of searching for the center of the area struck by the electron beam is given in Table 3. The numbers on the face of the foil correspond to the trial numbers in the table.

Table 3. Measurements of beam spot location

Trial	Count time (sec)	X-ray counts	X-ray rate (cts/sec)	100-keV counts	100-keV rate (cts/sec)
1	2548	259	0.10	79	0.031
2	1275	361	0.28	36	0.028
3	1700	1233	0.73	56	0.033
4	1500	1250	0.83	36	0.024
5	3796	3786	0.99	100	0.026
6	1800	655	0.36	44	0.024
7	2550	181	0.07	42	0.016

Figure 8 is a plot of the X-ray counts vs trial (location on foil) and it is evident that the true location of the center of the beam spot lies between locations #4 and #5.

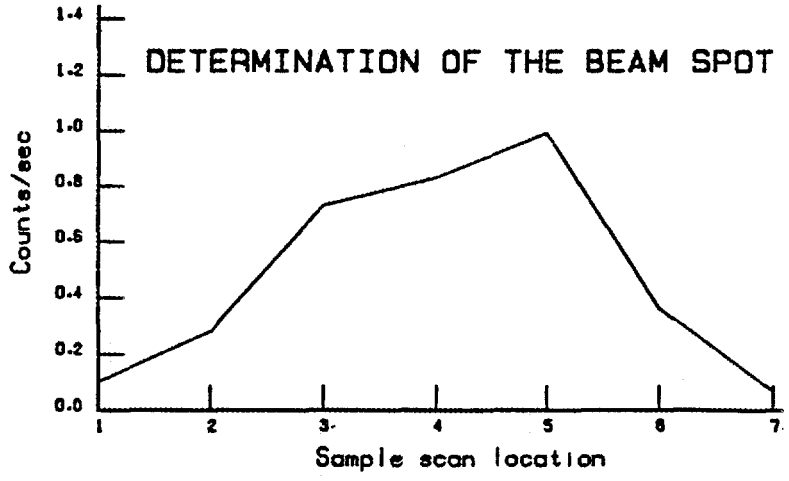

Fig. 8. Plot of X-ray counts per second versus sample "scan" location in an attempt to define the location of the actual beam spot.

A sample of the actual spectral data can be found in Figs. 9-11 on the following pages. The majority of the peaks are associated with tantalum isotopes, although the presence of the ^{180}Hf isomer with a gamma-ray energy of 443 keV is also evident.

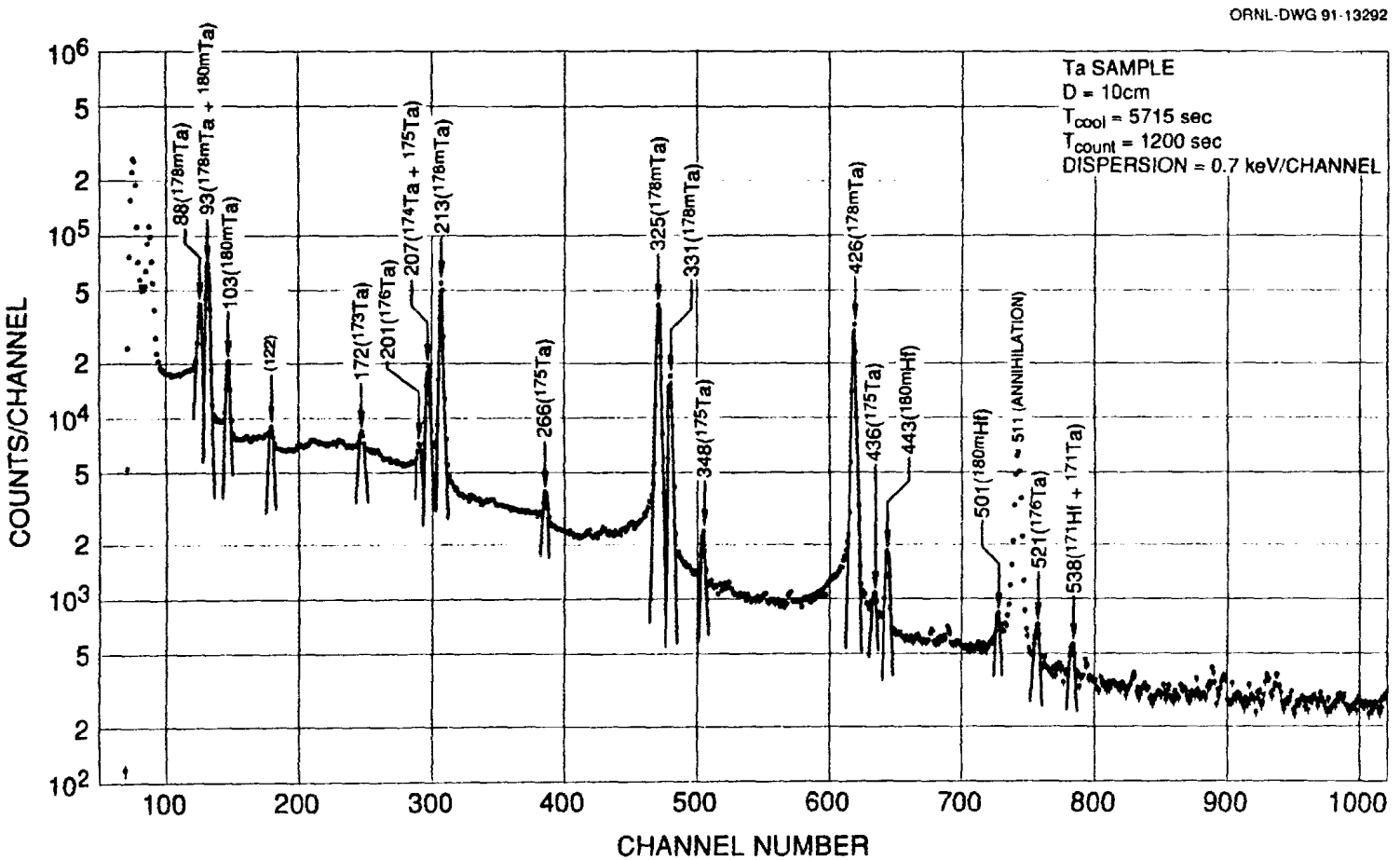

Fig. 9. Low-energy segment of the spectrum obtained commencing about 1.58 hours at the end of a 120-second irradiation of a ^{181}Ta foil by bremsstrahlung from the ORELA. Peaks are labelled with detected gamma-ray energy, in keV, and the assigned radioisotope.

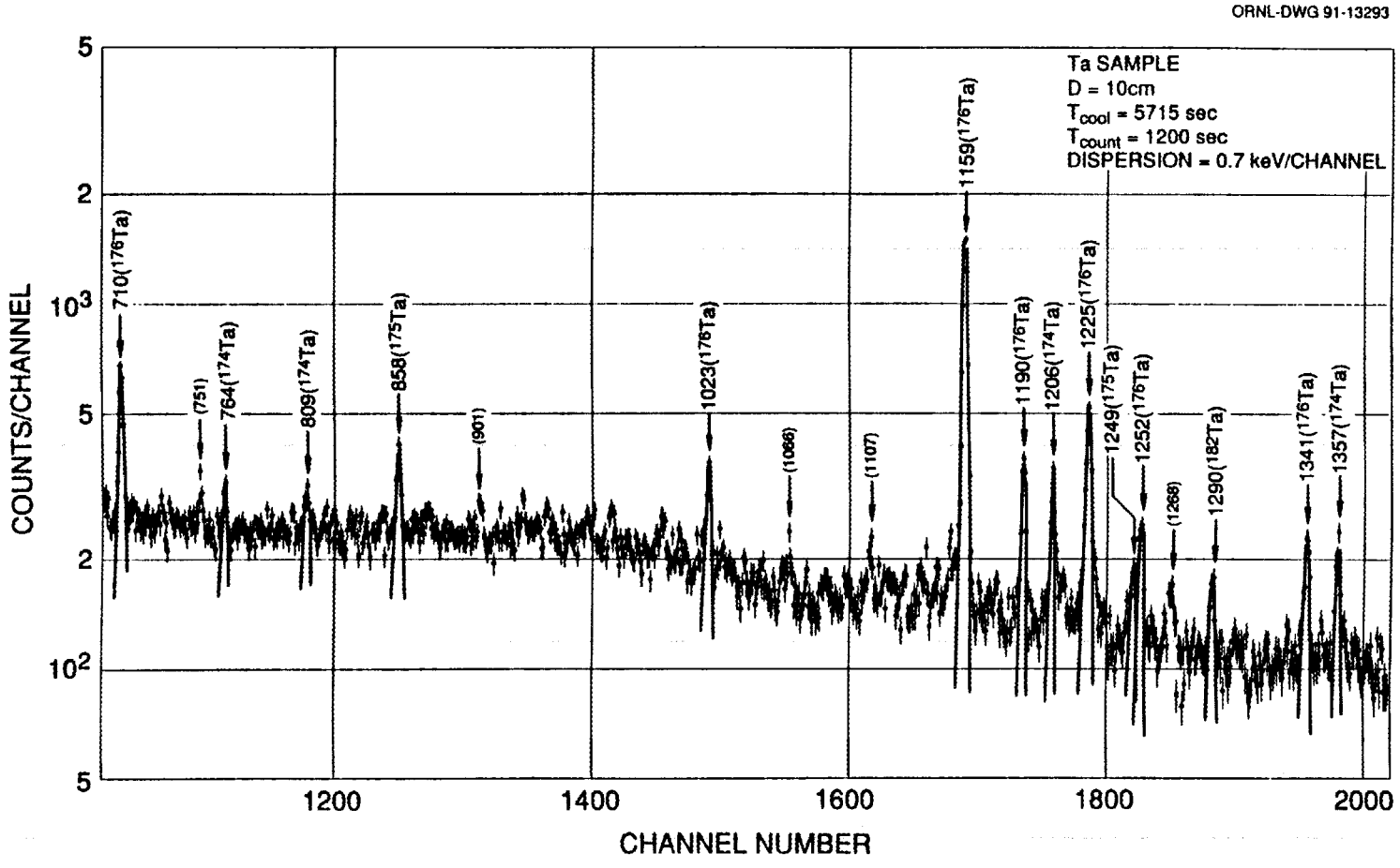

Fig. 10. Next larger-energy segment of the spectrum.

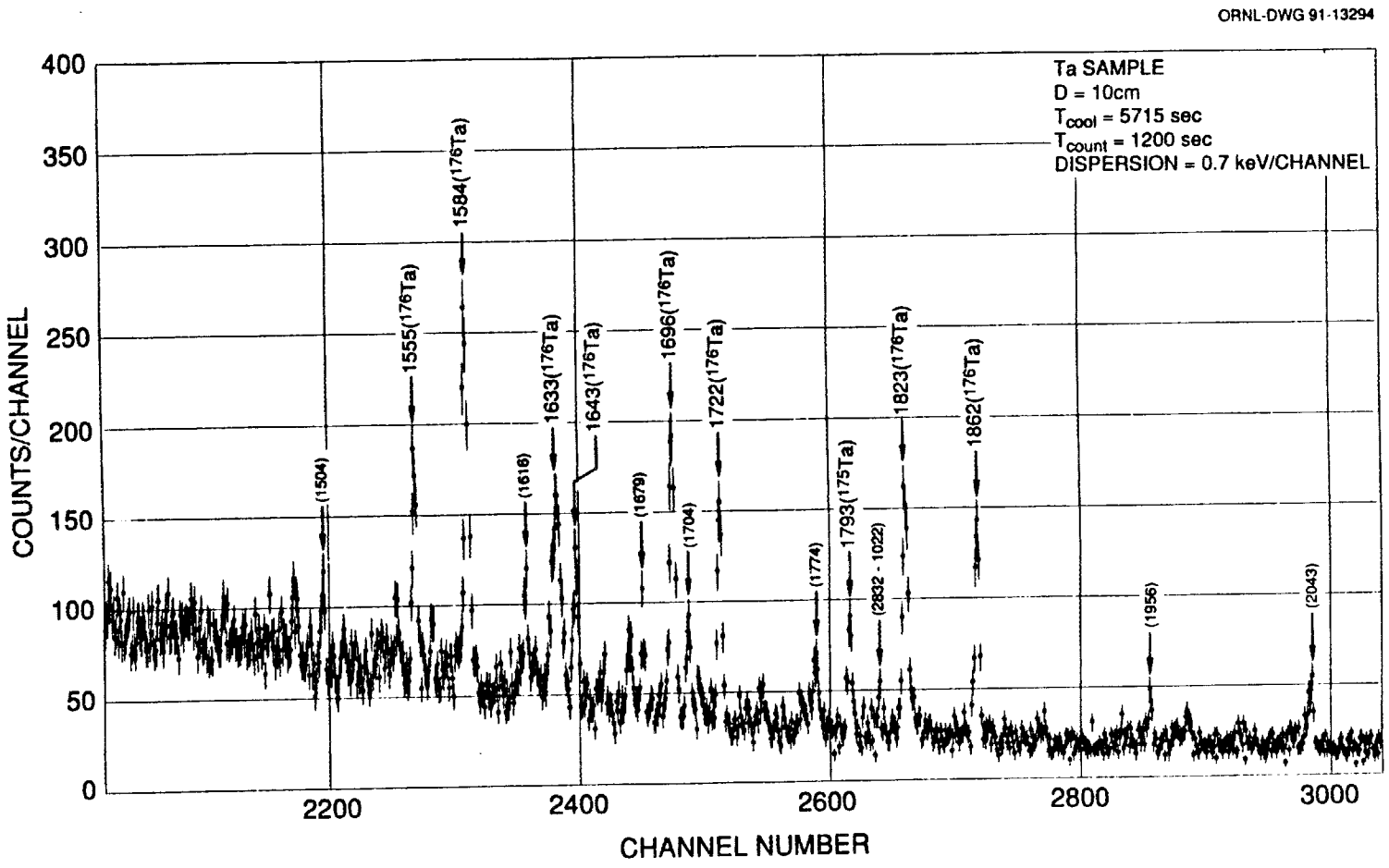

Fig. 11. Highest-energy portion of the spectrum. A double-escape peak is labelled with the responsible gamma-ray energy, in keV, minus 1022 keV.

4. DATA REDUCTION

The spectral data were first reduced using TPASS,[13] a gamma-ray spectrum analysis and isotope identification computer code. This code first determined peak yields and positions, and then used an input energy calibration to deduce gamma-ray energies and efficiency corrected yields. The TPASS program then used a table look-up procedure to assign gamma rays to appropriate decay transitions. The yields of the transitions which were observed were then combined to deduce the overall yield of each radioisotope. The TPASS results were checked for the cases of difficult peaks such as doublets using PLOTDATA,[14] a PC-interactive gamma-ray peak analysis program. Corrections were made to the detection efficiencies due to the offset of the beam spot on the sample. For the LEPS, the correction was 5%. For the Ge(Li) the correction was 2% for $D = 10$-cm data and 8% for the $D = 3$-cm data. Finally, corrections were made to the overall yield of each isotope for detector-efficiency and branching-ratio uncertainties. Uncertainties in gamma-ray branching ratios are taken from the literature.[15–20] The deduced yields of ten radionuclides produced during the irradiation are given in Table 4.

Table 4. Yields of isotopes created by Ta + γ reactions

Isotope	Half-life	E_γ (keV)	BR[a]	ΔBR (%)	Ref.[b]	Yield (atoms)
^{180}Ta	8.15 hrs	93.3	0.0428	4.2	15	$(1.005 \pm 0.055) \times 10^{11}$
^{180m}Hf	5.52 hrs	443.2	0.833	1.7	15	$(8.38 \pm 0.26) \times 10^{7}$
^{178}Ta	9.3 min	1350.6	0.0118	9.0	16	$(2.72 \pm 0.31) \times 10^{9}$
^{178m}Ta	2.4 hrs	426.4	0.969	2.0	16	$(1.11 \pm 0.08) \times 10^{9}$
^{177}Ta	56.6 hrs	113.0	0.072	10	17	$(2.51 \pm 0.38) \times 10^{9}$
^{176}Ta	8.1 hrs	1159.3	0.238	7.5	18	$(1.36 \pm 0.11) \times 10^{9}$
^{175}Ta	10.5 hrs	348.5	0.114	10	17	$(9.60 \pm 1.01) \times 10^{8}$
^{174}Ta	1.1 hrs	764.8	0.0126	8.7	19	$(4.24 \pm 0.46) \times 10^{8}$
^{173}Ta	3.6 hrs	172.2	0.175	9.7	20	$(1.79 \pm 0.19) \times 10^{8}$
^{172}Ta	37 min	1109.3	0.146	10	17	$(2.5 \pm 0.4) \times 10^{7}$

[a]Branching ratios (BR) are absolute values per decay.

[b]Ref. denotes the reference number where information on the isotope can be found.

Gamma rays chosen to represent decay of a given radionuclide did not always have the largest branching ratio following decay of that radioisotope. More important was to choose a gamma ray which was due only to the decay of interest.

Identification of particular gamma-ray peaks with a specific radionuclide decay relied not only on gamma-ray energy but also on the apparent decay rate of the yield. Therefore, as a part of the data reduction, half-lives of each nuclide identified

were determined by comparing values of counting rate and uncertainties vs cooling time for the yield of a gamma-ray characteristic of the decay of the isotope.[15–20] These data were analyzed using standard least-squares methodology[21] to obtain the "best-fit" half life for the radioisotope being studied. The results are shown in Table 5 and Figs. 12-21.

Table 5. Half-life determinations for various isotopes

Nuclide[a]	Gamma energy (keV)	Half life	
		Measured	Previous
^{180}Ta	93.3	(8.10 ± 0.02) hrs	8.152 hrs
^{180m}Hf	443.2	(6.05 ± 0.06) hrs	5.5 hrs
^{178}Ta	1350.6	(8.97 ± 0.71) min	9.31 min
^{178m}Ta	426.4	(2.58 ± 0.03) hrs	2.36 hrs
^{177}Ta	113.0	(57.8 ± 0.9) hrs	56.6 hrs
^{176}Ta	1159.3	(8.12 ± 0.06) hrs	8.09 hrs
^{175}Ta	348.5	(10.78 ± 0.11) hrs	10.5 hrs
^{174}Ta	764.8	(64 ± 12) min	70.8 min
^{173}Ta	172.2	(3.59 ± 0.12) hrs	3.14 hrs
^{172}Ta	1109.3	(46 ± 26) min	36.8 min

[a]References are the same as given in Table 4.

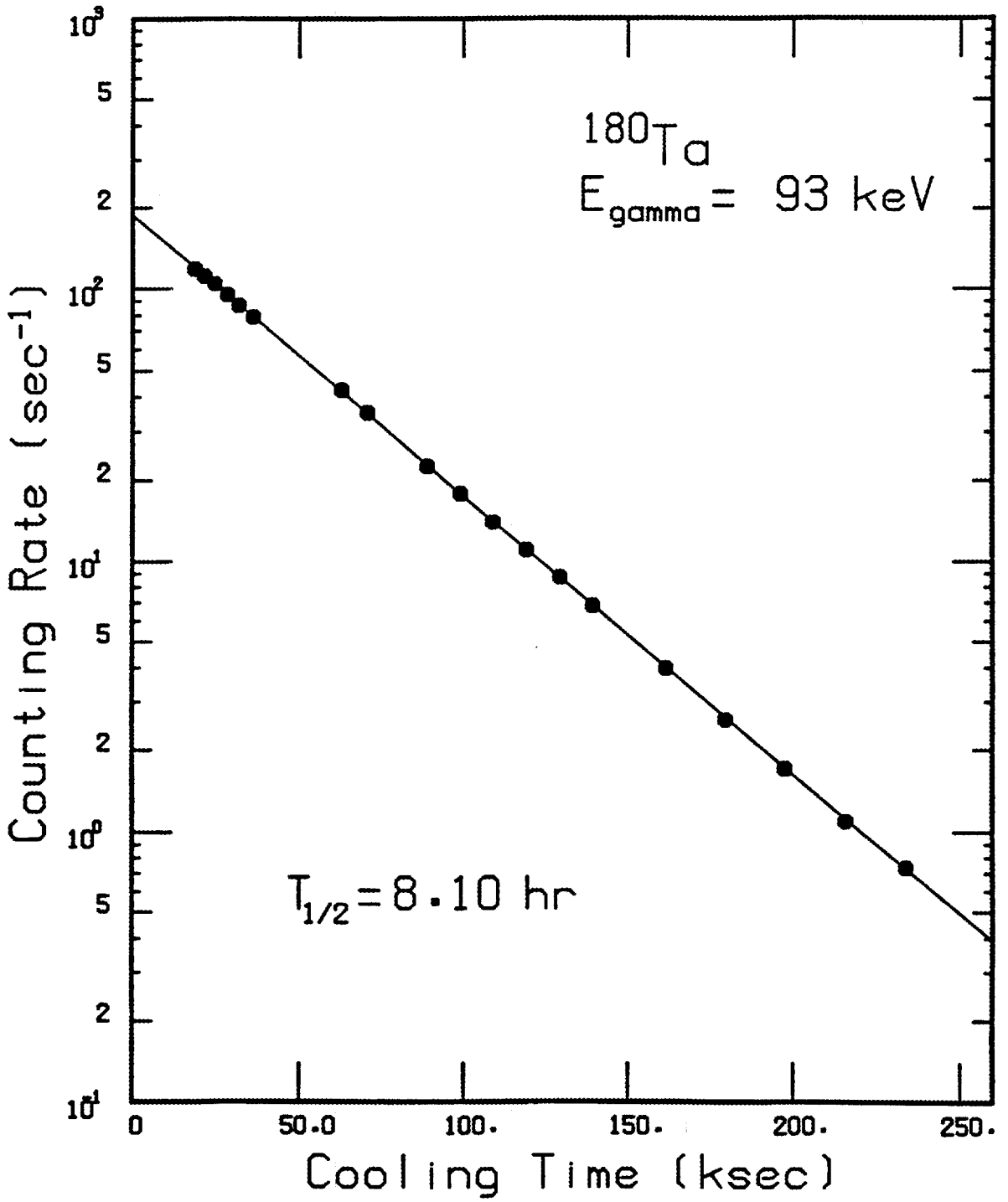

Fig. 12. Half life of ^{180}Ta deduced from the present experimental data for $E_\gamma = 93$ keV. The experimental data are shown as points and represent the computed counting rate of the peak corresponding to 93 keV in the experimental spectra corrected for dead-time effects but not for detector efficiency or the Ta decay branching ratio for this gamma ray. The deduced half life is indicated in the lower left portion of the figure and shown by the straight line. The present result of 8.10 ± 0.02 hr is in good agreement with the currently accepted value of 8.152 hr for the half life of this radioisotope.

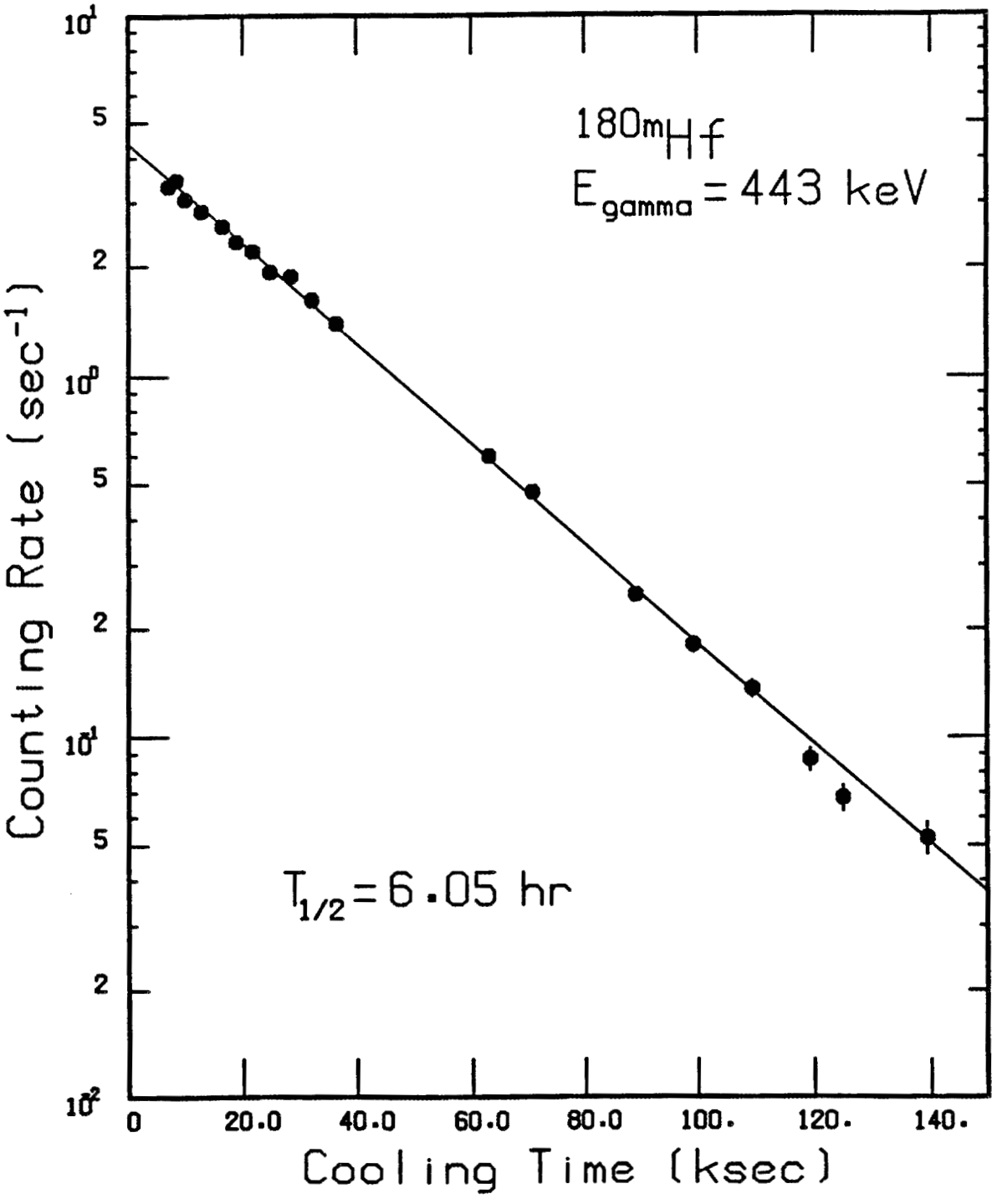

Fig. 13. Half life of ^{180m}Hf deduced from the present experimental data for $E_\gamma = 443$ keV. The experimental data are shown as points and represent the computed counting rate of the peak corresponding to 443 keV in the experimental spectra corrected for dead-time effects but not for detector efficiency or the Ta decay branching ratio for this gamma ray. The deduced half life is indicated in the lower left portion of the figure and shown by the straight line. The present result of 6.05 ± 0.06 hr does not agree with the currently accepted value of 5.5 ± 0.1 hr for the half life of this radioisotope. As discussed in the text, the present measurement may represent a definitive new measurement of this half-life.

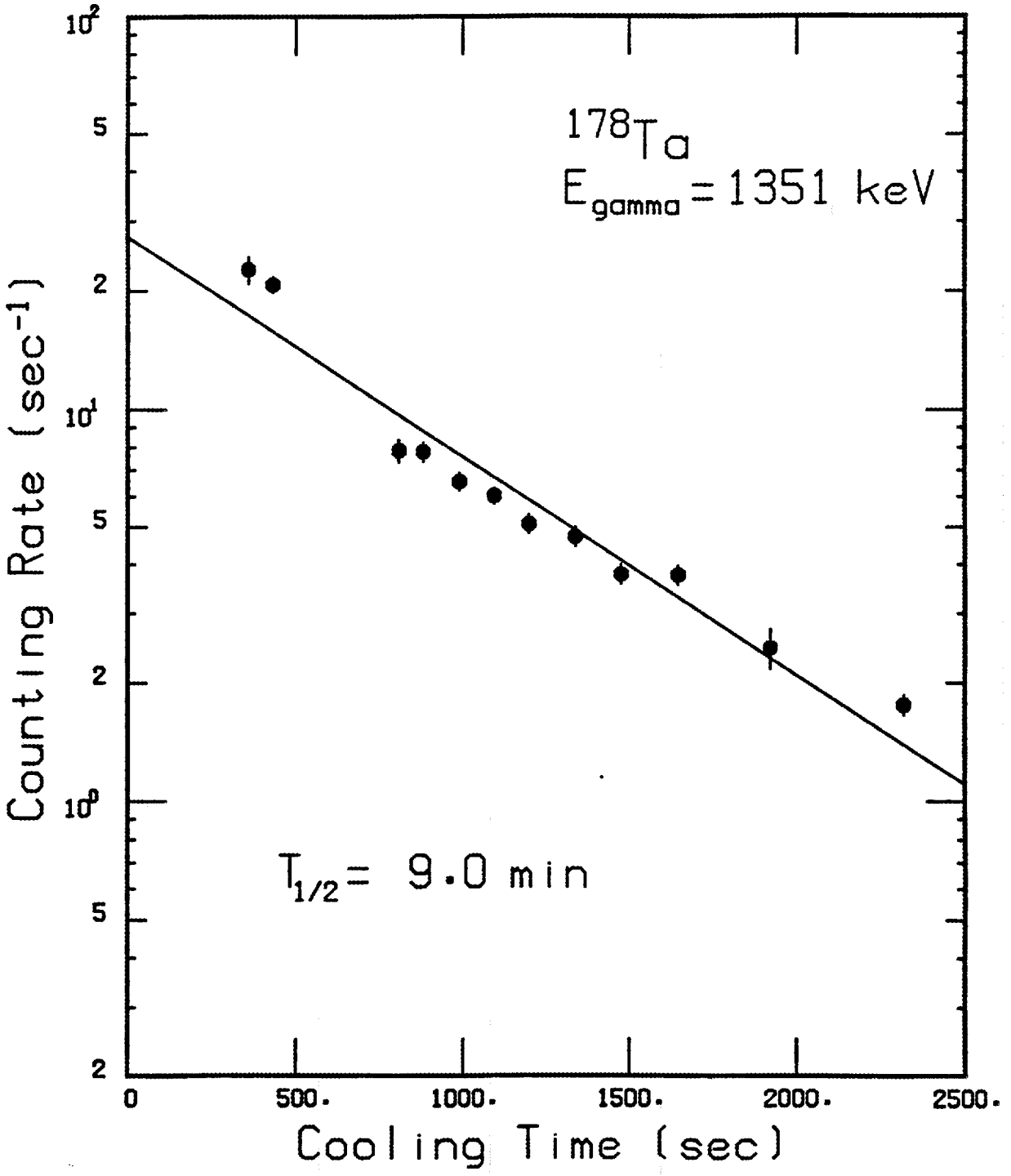

Fig. 14. Half life of ^{178}Ta deduced from the present experimental data for $E_\gamma = 1351$ keV. The experimental data are shown as points and represent the computed counting rate of the peak corresponding to 1351 keV in the experimental spectra corrected for dead-time effects but not for detector efficiency or the Ta decay branching ratio for this gamma ray. The deduced half life is indicated in the lower left portion of the figure and shown by the straight line. The present result of 9.0 ± 0.71 min is in good agreement with the currently accepted value of 9.31 min for the half life of this radioisotope.

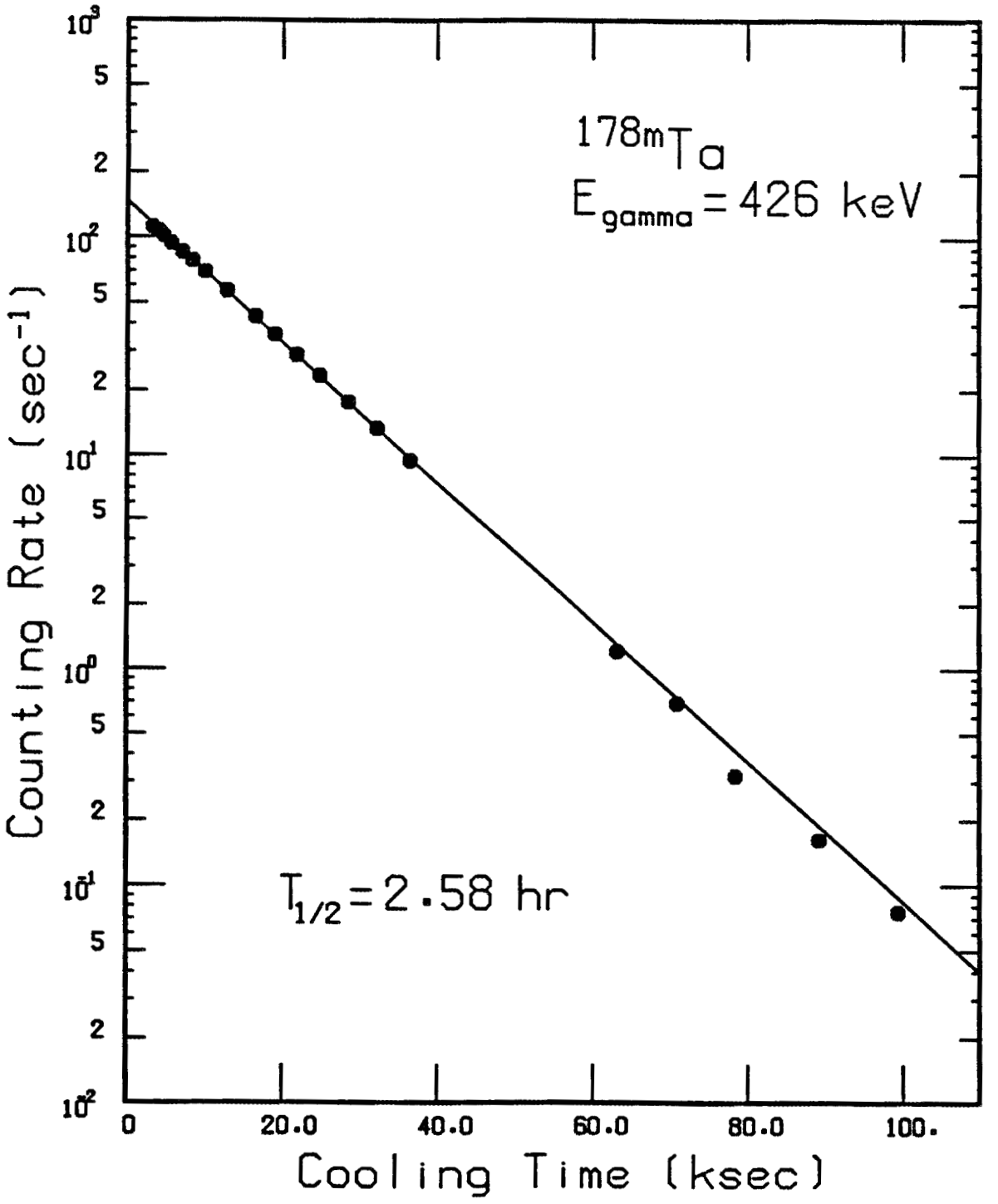

Fig. 15. Half life of ^{178m}Ta deduced from the present experimental data for $E_\gamma = 426$ keV. The experimental data are shown as points and represent the computed counting rate of the peak corresponding to 426 keV in the experimental spectra corrected for dead-time effects but not for detector efficiency or the Ta decay branching ratio for this gamma ray. The deduced half life is indicated in the lower left portion of the figure and shown by the straight line. The present result of 2.58 ± 0.03 hr does not agree well with the currently accepted value of 2.36 hr for the half life of this radioisotope. Further analysis of the present data is indicated by the disagreements noted for cooling times >60 ksec. It is not anticipated, however, that the observed disagreement, being on the order of 9%, would substantially affect the determination of radioisotope yield as presented in the text.

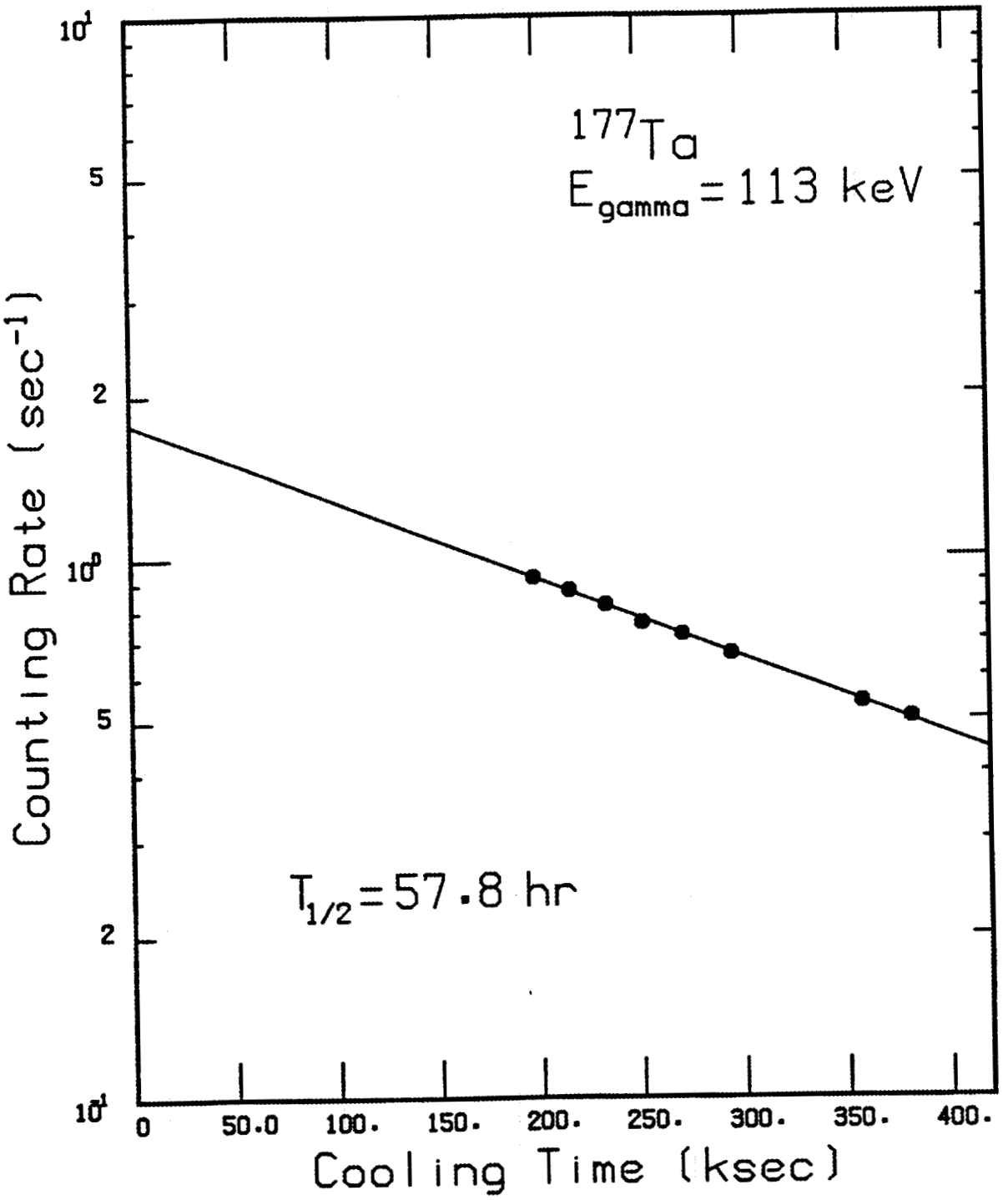

Fig. 16. Half life of ^{177}Ta deduced from the present experimental data for $E_\gamma = 113$ keV. The experimental data are shown as points and represent the computed counting rate of the peak corresponding to 113 keV in the experimental spectra corrected for dead-time effects but not for detector efficiency or the Ta decay branching ratio for this gamma ray. The deduced half life is indicated in the lower left portion of the figure and shown by the straight line. The present result of 57.8 ± 0.9 hr is in good agreement with the currently accepted value of 56.6 hr for the half life of this radioisotope.

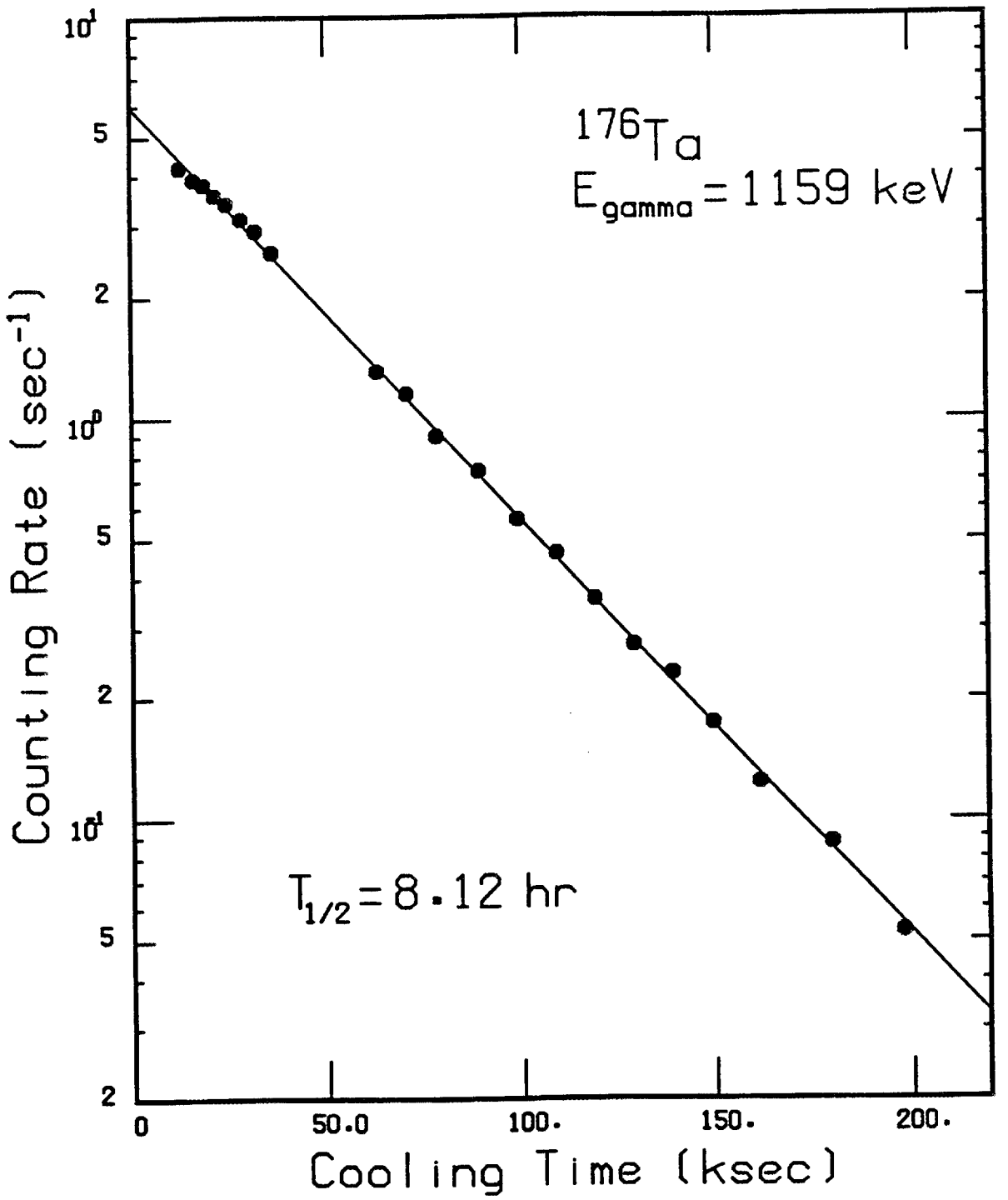

Fig. 17. Half life of ^{176}Ta deduced from the present experimental data for $E_\gamma = 1159$ keV. The experimental data are shown as points and represent the computed counting rate of the peak corresponding to 1159 keV in the experimental spectra corrected for dead-time effects but not for detector efficiency or the Ta decay branching ratio for this gamma ray. The deduced half life is indicated in the lower left portion of the figure and shown by the straight line. The present result of 8.12 ± 0.06 hr is in very good agreement with the currently accepted value of 8.09 hr for the half life of this radioisotope.

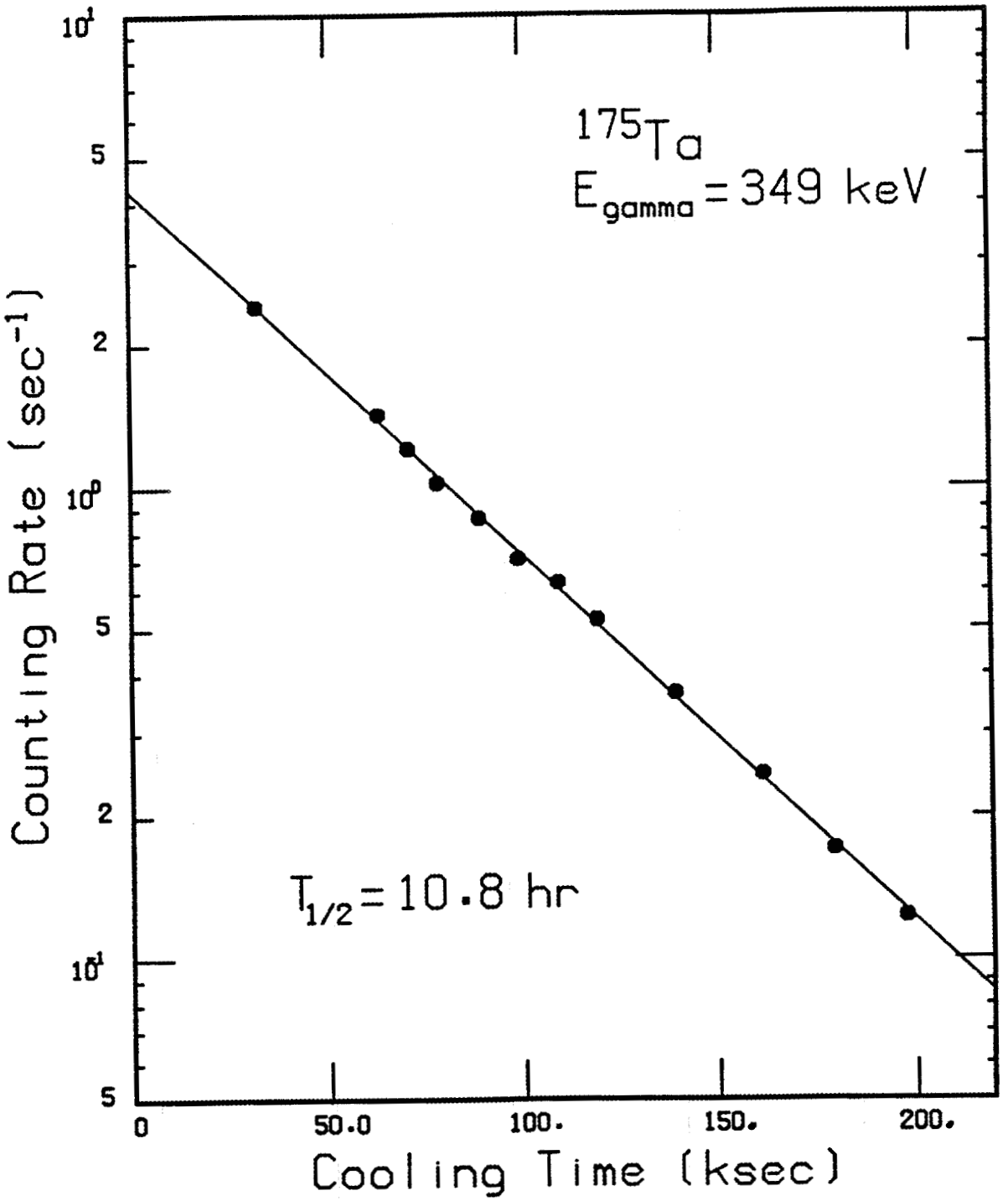

Fig. 18. Half life of ^{175}Ta deduced from the present experimental data for $E_\gamma = 349$ keV. The experimental data are shown as points and represent the computed counting rate of the peak corresponding to 349 keV in the experimental spectra corrected for dead-time effects but not for detector efficiency or the Ta decay branching ratio for this gamma ray. The deduced half life is indicated in the lower left portion of the figure and shown by the straight line. The present result of 10.8 ± 0.11 hr is in very good agreement with the currently accepted value of 10.5 ± 0.2 hr for the half life of this radioisotope.

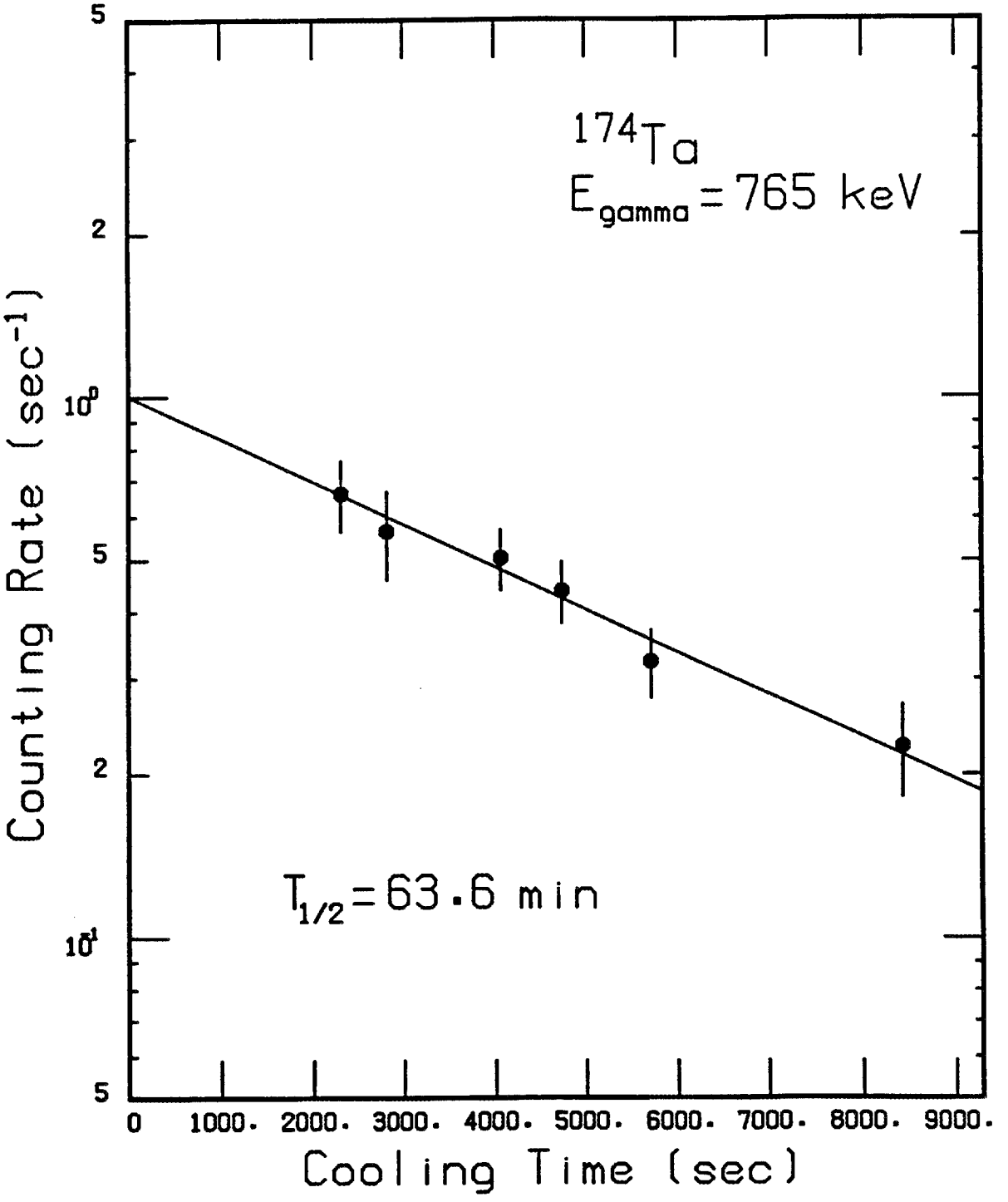

Fig. 19. Half life of ^{174}Ta deduced from the present experimental data for $E_\gamma = 765$ keV. The experimental data are shown as points and represent the computed counting rate of the peak corresponding to 765 keV in the experimental spectra corrected for dead-time effects but not for detector efficiency or the Ta decay branching ratio for this gamma ray. The deduced half life is indicated in the lower left portion of the figure and shown by the straight line. The present result of 63.6 ± 12 min is in very good agreement with the currently accepted value of 71 min for the half life of this radioisotope.

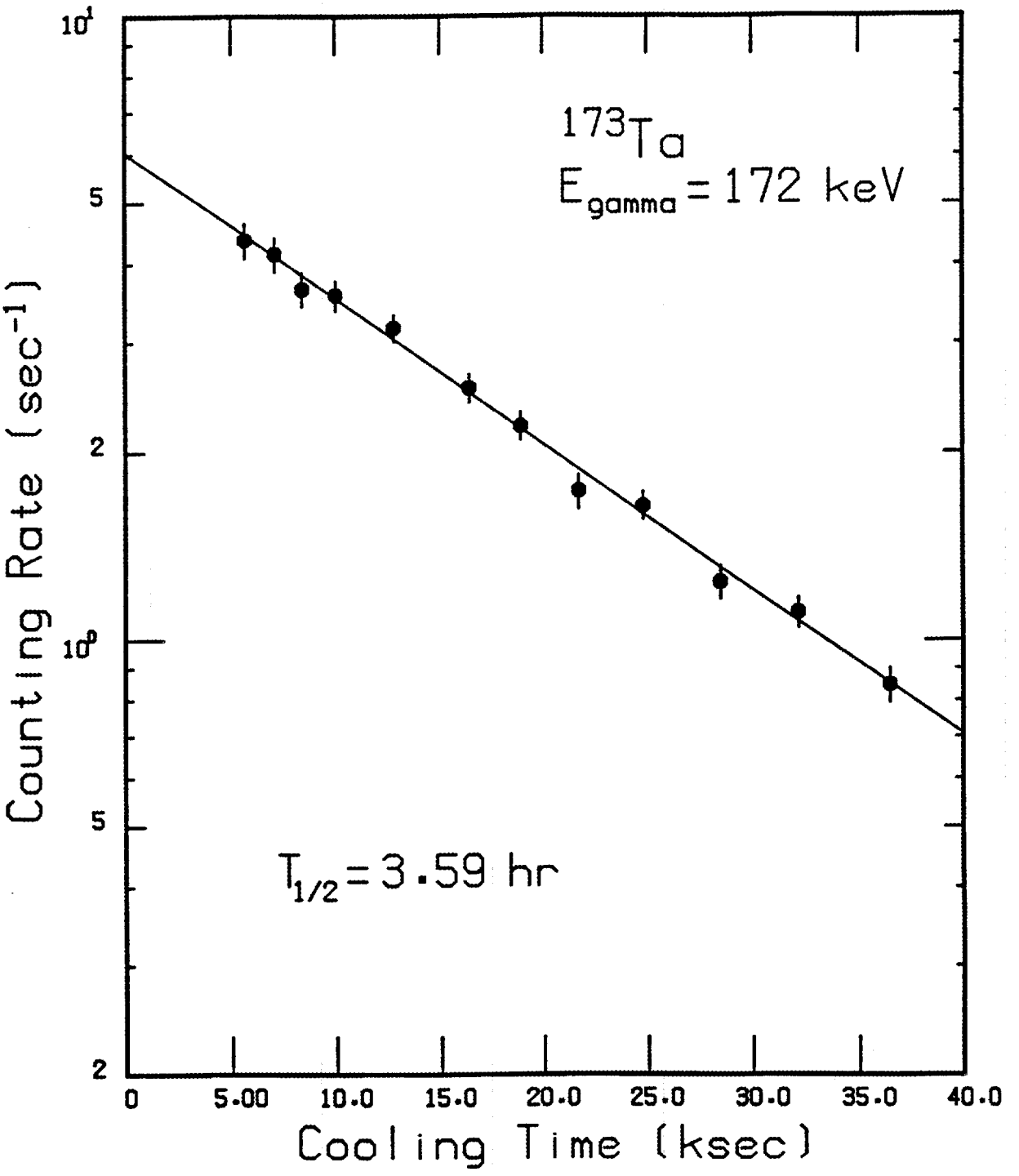

Fig. 20. Half life of ^{173}Ta deduced from the present experimental data for $E_\gamma = 172$ keV. The experimental data are shown as points and represent the computed counting rate of the peak corresponding to 172 keV in the experimental spectra corrected for dead-time effects but not for detector efficiency or the Ta decay branching ratio for this gamma ray. The deduced half life is indicated in the lower left portion of the figure and shown by the straight line. The present result of 3.59 ± 0.12 hr does not agree well with the currently accepted value of 3.14 hr for the half life of this radioisotope. As discussed in the text further study is planned on the present experimental results.

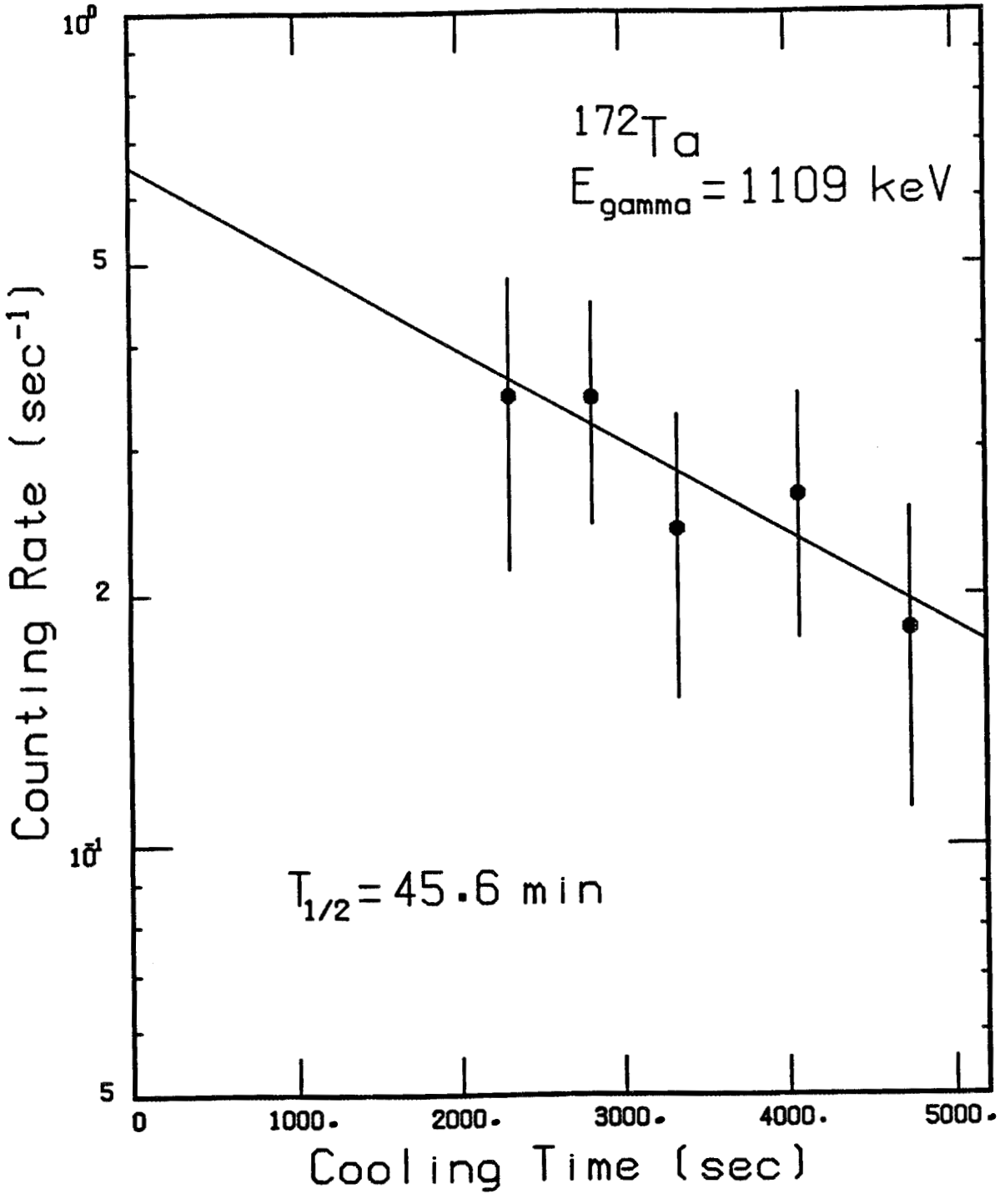

Fig. 21. Half life of ^{172}Ta deduced from the present experimental data for E_γ = 1109 keV. The experimental data are shown as points and represent the computed counting rate of the peak corresponding to 1109 keV in the experimental spectra corrected for dead-time effects but not for detector efficiency or the Ta decay branching ratio for this gamma ray. The deduced half life is indicated in the lower left portion of the figure and shown by the straight line. The present result of 46 ± 26 min is consistent with the currently accepted value of 36.8 min for the half life of this radioisotope.

5. DISCUSSION OF RESULTS

The half-life determinations for ^{180}Ta, ^{178}Ta, ^{176}Ta, ^{174}Ta, and ^{172}Ta agree well with previous measurements.[15–19] The half-life determination for ^{177}Ta is close to the previous value[17] and certainly within two standard deviations. A better value may have been obtained if points corresponding to shorter cooling times had also been obtained. The half-life of ^{175}Ta is also close enough to the previously measured value[17] to be in satisfactory agreement.

The ^{180m}Hf analysis is interesting in that it may suggest a new value for this half-life. We are confident in this suggestion since ^{180m}Hf has nothing to "feed" it and the gamma ray examined (443 keV) had no interference from other similar energy gamma rays. The presently measured half life for ^{173}Ta also tends to fit the criteria used to establish the validity of the presently measured ^{180m}Hf half-life. However, it is apparent from Fig. 20 that the data for ^{173}Ta are more erratic than in the case of the ^{180m}Hf. Therefore, while the numbers may indicate a new determination of the half-life, we suggest that further analysis is required to obtain a definitive answer. The ^{178m}Ta half life is not in agreement with previously measured values. Figure 15 shows the relevant data and the data suggest that the gamma-ray peak in the spectral data may have another, yet to be identified, contribution to its yield. However, the additional contribution, if there is one, is not large and should have essentially no impact on the reported yield in Table 4 for the amount of ^{178m}Ta produced by the irradiation.

The results displayed in Table 4 indicate that nearly all of the reaction products are Ta, the most abundant being ^{180}Ta. As expected, the yields of the various tantalum isotopes created during the irradiation decrease with decreasing neutron number. Thus, the yield of the ^{172}Ta is less than that of ^{173}Ta, which is less than ^{174}Ta, etc. These results are not surprising since the yield of the incident photon spectrum (bremsstrahlung) decreases with increasing photon energy. Thus, the total number of incident photons having energies in excess of the reaction threshold energy (see Table 1) decreases as the value of the reaction threshold increases.

Another interesting observation is that the yields did not decrease successively by the anticipated factor of 4. Instead, for yield determinations down to ^{173}Ta the decrease between successive isotopes was no more than 2.4. This result is, however, approximately consistent with the overall $\approx 1/E$ shape of the bremsstrahlung. One aspect of the results that does demand further study is the factor of seven difference from the yield of the ^{173}Ta to the yield of ^{172}Ta. From Table 1 the Q-value for the $(\gamma, 9n)$ reaction is 69.6 ± 0.20 MeV, which lies nearly in the middle of the bremsstrahlung energy spectrum. It can be seen in Fig. 1 that the curve is not steeply sloping at this point. Thus, this decrease in yield from ^{173}Ta to ^{172}Ta is larger than expected just from the shape of the bremsstrahlung curve.

It is also interesting to note that previous experimental work at this laboratory[22] on photon irradiation of elemental Ni shows that the preferred reaction mechanism was the $(\gamma, 1p)$ reaction. In this experiment with tantalum, the yield of ^{180m}Hf corresponding to the $(\gamma, 1p)$ reaction is substantially smaller than the yield of the

^{180}Ta which results from the $(\gamma, 1n)$ reaction. For tantalum the preferred reaction mechanism is $(\gamma, 1n)$.

Finally, it was observed that a large amount of thermal-neutron-induced ^{182}Ta was present in nearly constant amounts throughout the sample. The production of this radionuclide is not due to any $(\gamma, xn\ yp)$ reaction with tantalum, but instead is a result of the ORELA target being a strong source of low-energy neutrons. ^{182}Ta has a half-life of 114.5 days, and its presence was in such large amounts that it interfered with analysis of decay gamma rays from other long-lived radionuclides produced by photonuclear reactions during the irradiation.

6. CONCLUSION

The study of radionuclides created in the electron-bombardment of element ^{181}Ta has had the first purpose of determining types and yields of each isotope created. The results give both qualitative and quantitative information on the overall production yields of ten radionuclides covering a mass range of 9 units. As stated previously in the introduction, this information is useful for the purposes of both basic physics and applied science. In an applied sense, these yield determinations provide a basis for accurate assessments of what kind (and how much) of a particular radiosotope will be present in the ORELA target. All of the tantalum isotopes created by (γ, xn) reactions have fairly short half-lives and would not be expected to be present in the ORELA target in any significant quantities after several days of cooling. Since all the tantalum isotopes created in the irradiation with the exception of very long-lived ^{180}Ta decay, the production of long-lived radionuclides such as ^{172}Hf, ^{175}Hf, etc., is to be expected. The amounts of these, however, are small in comparison to the amount of ^{182}Ta produced. For maintenance and, ultimately, disposal purposes, the greatest concern should be with the amount of ^{182}Ta present in the ORELA target.

The analysis of the half-lives of the ten radionuclides also revealed useful information. The previous half-life measurements for five of the radionuclides[15–19] (^{180}Ta, ^{178}Ta, ^{176}Ta, ^{174}Ta, and ^{172}Ta) were supported by our measurements. Half-life measurements ^{175}Ta and ^{177}Ta were interpreted as being supportive of previous measurements[17] due to the fact that they were within two standard deviations. The last three half-life measurements for ^{178m}Ta, ^{180m}Hf, and ^{173}Ta were found to disagree with measurements found in the literature.[15,16,19] The data suggest a new determination of the half-life for ^{180m}Hf as $6.05 \pm 0.06 hr$, or about 10% longer than the currently adopted value for this half life. The erratic nature of the data in Fig. 20 suggests that further analysis on ^{173}Ta is needed. The only measurement which appeared to have a problem was that for ^{178m}Ta. The possibility of an unknown contribution necessitates further investigation before a definitive conclusion can be reached.

As a final note, future experiments intending to study the $(\gamma, xn\ yp)$ reaction in greater detail are advised to use an experimental configuration in which capture effects due to neutrons produced by the Ta target are minimized, thus revealing the presence of any long-lived radionuclides created during irradiation. Placing the sample as far away from the target as possible is strongly recommended.

REFERENCES

1. R. G. Alsmiller, Jr., T. A. Gabriel, and M. P. Guthrie, *Nuclear Science and Engineering* **40**, 365 (1970).
2. C. E. Burgart, E. A. Straker, T. A. Love, and R. M. Freestone, Jr., *Nucl. Sci. Eng.* **42**, 421 (1970).
3. R. Borgere, H. Beil, and A. Veyssiere, *Nucl. Phys.* **A121**, 463 (1968).
4. K. Masumoto, T. Kato, and N. Suzuki, *Nucl. Instruments and Methods* **157**, 567 (1978).
5. T. A. Lewis, (private communication).
6. *Studies in Penetration of Charged Particles in Matter*, National Academy of Sciences – National Research Council Publication 1133 (Washington, D.C., 1964).
7. H. E. Johns, L. Katz, R. A. Douglass, and R.N.H. Haslam, *Physical Review* **80**, 1062 (1950).
8. A. S. Penfold and J. E. Leiss, *Phys. Rev.* **114**, 1332 (1959).
9. A. H. Wapstra and G. Audi, *Nucl. Phys.* **A432**, 1 (1985).
10. F. Walker, D. G. Miller, and F. Feiner, *Chart of the Nuclides*, (General Electric Co., 1984), Thirteenth Edition, p. 41.
11. J. E. Turner, *Atoms, Radiation, and Radiation Protection*, (Permagon Press, New York, 1986), p. 93, 123.
12. D. Halliday and R. Resnick, *Fundamentals of Physics*, (John Wiley and Sons, Inc., 1988), Third Edition, p. 466, 472.
13. J. K. Dickens, *TPASS, A Gamma-Ray Spectrum Analysis and Isotope Identification Computer Code*, Oak Ridge National Laboratory Report No. ORNL-5732 (1981).
14. R. L. Bywater, Jr., *Gamma-Ray Production Cross Sections for 0.9 to 20 MeV Neutron Interactions with* ^{10}B, Oak Ridge National Laboratory Report No. ORNL/TM-10191 (1986).
15. E. Browne, *Nucl. Data Sheets* **52**, 127 (1987).
16. E. Browne, *Nucl. Data Sheets* **54**, 199 (1988).
17. U. Reus and W. Westmeier, *Atomic and Nuclear Data Tables* **29**, 193 (1983).
18. E. Browne, *Nucl. Data Sheets* **60**, 227 (1990).
19. E. Browne, *Nucl. Data Sheets* **41**, 511 (1988).
20. V. S. Shirley, *Nucl. Data Sheets* **54**, 589 (1988).
21. J. K. Dickens, *Radiochem. Radioanal. Lett.* **39**, 107 (1979).
22. J. K. Dickens, *Study of Radionuclides Created by* $^{nat}Ni(\gamma, xn\ yp)$ *Reactions for Bremsstrahlung Photons Produced by 140-MeV Electrons*, Oak Ridge National Laboratory report No. ORNL/TM-9764 (1986).

INTERNAL DISTRIBUTION

1. R. G. Alsmiller, Jr.
2. B. R. Appleton
3–7. J. K. Dickens
8. T. A. Gabriel
9. J. A. Harvey
10. D. M. Hetrick
11. D. T. Ingersoll
12–16. D. C. Larson
17. T. A. Lewis
18. R. W. Peelle
19. C. R. Richmond
20. R. R. Spencer
21. K. M. Wallace
22. R. C. Ward
23. R. W. Brockett (consultant)
24. J. J. Dorning (consultant)
25. J. E. Leiss (consultant)
26. N. Moray (consultant)
27. M. F. Wheeler (consultant)
28. EPMD Reports Office
29–30. Laboratory Records Department
31. Laboratory Records, ORNL-RC
32. Document Reference Section
33. Central Research Library
34. ORNL Patent Section

EXTERNAL DISTRIBUTION

35. L. Barker, Post Secondary Programs Division, Office of University and Science Education, ER 82, Forrestal Bldg., Washington, D. C. 20585
36. Jerome L. Duggan, Department of Physics, North Texas State University, Denton, Texas 76203
37. R. A. Meyer, Division of Nuclear Physics, ER 23/GTN, U. S. Department of Energy, Washington, D. C. 20585
38–42. Matthew A. Miller, HCR69, Box 53B, Shell Lake, WI 54871
43. R. Stevens, Office of University and Science Education, ER 80, Forrestal Bldg., Washington, D. C. 20585
44. Chairman, Department of Physics, University of Wisconsin, River Falls, WI 54022
45. S. L. Whetstone, Division of Nuclear Physics, ER 23/GTN, U. S. Department of Energy, Washington, D. C. 20585
46. R. Wiesenhuegel, Director, Student Programs, Science/Engineering Education Division, Oak Ridge Associated Universities, Post Office Box 117, Oak Ridge, TN 37831-0117
47. Office of the Assistant Manager for Energy Research and Development, U. S. Department of Energy, Oak Ridge Operations, P. O. Box 2008, Oak Ridge, TN 37831
48–57. Office of Scientific and Technical Information, P. O. Box 62, Oak Ridge, TN 37831